

SYNTHESIS AND CHARACTERIZATION OF TIME-RESOLVED FLUORESCENCE  
PROBES FOR THE POTENTIAL DETECTION AND IMPROVED STUDY OF MELANOMA  
CANCER

A Thesis

Presented to the faculty of the Graduate School of  
Western Carolina University in partial fulfillment of the  
requirements for the degree of Master of Science in  
Chemistry.

By

Seth Sedberry

Advisor: Dr. Brian Dinkelmeyer,  
Associate Professor, Organic Chemistry,  
Department of Chemistry & Physics

August 2016

## ACKNOWLEDGEMENTS

I would like to thank my sister Jenna for balancing friendship with the gradual destruction of my ego, my parents for their support, my grandparents Lynn and Linda for always pushing me to aim higher, and Dr. Krista Wilson and the Wingate University Department of Chemistry and Physics for their instruction and inspiration. I would also like to acknowledge the numerous friends, family members, and brothers who have offered immeasurable amounts of their companionship and support, they number too many to name individually but are certainly in my heart. These influences have been very important for my growth and I hold them in the highest esteem. I would also like to thank my research committee for their continuous contributions, Dr. Brian Dinkelmeyer in particular. Their superb assistance has allowed me the proper environment to grow and study. Thanks to their efforts, my time at Western Carolina University has been rich and joyful, leaving me with the desire to continue my scientific education. YITBOS

## TABLE OF CONTENTS

|  |           |
|--|-----------|
| List of Abbreviations .....  | vii       |
| List of Figures .....  | viii      |
| List of Schemes .....  | x         |
| List of Tables .....   | x         |
| <b>ABSTRACT</b> .....  | <b>ix</b> |
| <b>CHAPTER 1: INTRODUCTION</b> .....   | <b>1</b>  |
| 1.1 PROBLEM STATEMENT .....  | 1         |
| 1.2 BACKGROUND .....   | 1         |
| 1.2.1 MALIGNANT MELANOMA AND G-PROTEIN COUPLED RECEPTORS .....                                       | 1         |
| 1.2.2 LANTHANIDE AND LIGAND CHEMISTRY .....  | 5         |
| 1.3 OBJECTIVES .....   | 7         |
| <b>CHAPTER 2: EXPERIMENTAL</b> .....   | <b>12</b> |
| 2.1 MATERIALS AND INSTRUMENTATION .....  | 12        |
| 2.1.1 FOURIER TRANSFORM INFRARED SPECTROSCOPY .....  | 12        |
| 2.1.2 NUCLEAR MAGNETIC RESONANCE SPECTROSCOPY .....  | 12        |
| 2.1.3 UV-VISIBLE ABSORPTION SPECTROSCOPY .....   | 13        |
| 2.1.4 FLUORESCENCE SPECTROSCOPY .....  | 13        |
| 2.1.5 GAS CHROMATOGRAPHY .....   | 13        |
| 2.1.6 LIQUID CHROMOTOGRAPHY .....  | 13        |
| 2.2 FUNCTIONALIZED PHENANTHROLINE LIGAND AND $\text{Eu}^{3+}$ COMPLEX SYNTHESIS .....                | 14        |
| 2.2.1 PREPARATION OF 5-NITRO-1,10-PHENANTHROLINE .....   | 14        |
| 2.2.2 SYNTHESIS OF 5-AMINO-1,10-PHENANTHROLINE .....   | 15        |
| 2.2.3 SYNTHESIS OF $\text{Eu}(\text{TTA})_3 \cdot 2\text{H}_2\text{O}$ .....                         | 16        |
| 2.2.4 SYNTHESIS OF 1,10-PHENANTHROLINE – $\text{Eu}(\text{TTA})_3$ COMPLEX .....                     | 17        |
| 2.2.5 SYNTHESIS OF 5-NITRO-1,10-PHENANTHROLINE – $\text{Eu}(\text{TTA})_3$ COMPLEX .....             | 18        |
| 2.2.6 SYNTHESIS OF 5-AMINO-1,10-PHENANTHROLINE – $\text{Eu}(\text{TTA})_3$ COMPLEX .....             | 19        |
| 2.3 POLYETHYLENE GLYCOL LINKER SYNTHESIS .....   | 20        |
| 2.3.1 SYNTHESIS OF TERT-BUTYL 17-HYDROXY-19,19-DIMETHYL-3,6,9,12,15,18-<br>HEXAOCOSANOATE .....      | 20        |
| 2.3.2 SYNTHESIS OF 2-HYDROXY-1 $\lambda^3$ ,4,7,10,13,16-HEXAOXAOCTADEC-1-YN-18-OIC ACID .....       | 21        |
| 2.3.3 SYNTHESIS OF 2-CHLORO-1 $\lambda^3$ ,4,7,10,13,16-HEXAOXAOCTADEX-1-YN-18-OYL<br>CHLORIDE ..... | 22        |
| 2.4 PEPTIDE SYNTHESIS .....  | 23        |
| 2.4.1 MELANOCYTE STIMULATING HORMONE (4) - PG .....  | 23        |
| <b>CHAPTER 3: RESULTS AND DISCUSSION</b> .....   | <b>25</b> |
| 3.1 PHENANTHROLINE LIGAND AND $\text{Eu}^{3+}$ COMPLEXES .....                                       | 25        |
| 3.1.1 SYNTHESIS AND CHARACTERIZATION .....   | 25        |
| 3.1.2 ULTRAVIOLET-VISIBLE ABSORPTION/ FLUORESCENT EMISSION STUDIES .....                             | 27        |
| 3.2 POLYETHYLENE GLYCOL LINKER .....   | 29        |

|   |           |
|---|-----------|
| 3.2.1 SYNTHESIS AND CHARACTERIZATION .....          | 29        |
| 3.2.2 GCMS AND HPLC STUDIES .....                   | 30        |
| 3.3 MELANOCYTE STIMULATING HORMONE (4) – PG.....    | 31        |
| 3.3.1 SOLID PHASE SYNTHESIS & CHARACTERIZATION..... | 31        |
| 3.4 CONCLUSION .....                                | 33        |
| 3.5 FUTURE WORK.....                                | 34        |
| <b>SUPPLEMENTAL MATERIAL.....</b>                   | <b>35</b> |
| <b>APPENDIX A - PERMISSIONS.....</b>                | <b>54</b> |
| <b>REFERENCES.....</b>                              | <b>55</b> |

## LIST OF ABBREVIATIONS

|        |   |
|--------|---|
| ATR    | Attenuated total reflectance                |
| MSH    | Melanocyte stimulating hormone              |
| HPLC   | High pressure liquid chromatography         |
| GCMS   | Gas chromatography mass spectroscopy        |
| LCMS   | Liquid chromatography mass spectroscopy     |
| FTIR   | Fourier transform infrared spectroscopy     |
| GPCR   | G-protein coupled receptor                  |
| NMR    | Nuclear magnetic resonance spectroscopy     |
| UV-Vis | Ultraviolet-Visible absorption spectroscopy |
| TFA    | Trifluoroacetic acid                        |
| DCM    | Dichloromethane                             |

## LIST OF FIGURES

|   |    |
|---|----|
| Figure 1: Location of melanocyte and melanin production in the skin .....   | 2  |
| Figure 2: A G-Protein Coupled Receptor activating a cell's signaling pathway through the presence of an agonist.....                            | 3  |
| Figure 3: The “Antenna Effect” .....  | 5  |
| Figure 4: Visualization of a Stoke's Shift.....   | 6  |
| Figure 5: Three component design of the proposed molecule.....  | 7  |
| Figure 6: MSH (4)-PG .....  | 11 |
| Figure 7: Melanocyte stimulating hormone (4) –PG .....  | 23 |
| Figure 8: Lanthanide complex UV-Vis absorbance.....   | 28 |
| Figure 9: Lanthanide complex fluorescent emission .....   | 28 |
| Figure 10: Melanocyte Stimulating Hormone (4) –PG.....  | 31 |
| Figure 11: LCMS of MSH (4) –PG .....  | 32 |
| Figure 12: Mass Spectra of MSH (4) –PG.....   | 32 |
| Figure 13: HPLC of MSH (4) –PG .....  | 33 |
| Figure 14: <sup>1</sup> H NMR spectrum of 5-Nitro-1,10-Phenanthroline in CDCl <sub>3</sub> .....  | 35 |
| Figure 15: Zoomed <sup>1</sup> H NMR spectrum of 5-Nitro-1,10-Phenanthroline in CDCl <sub>3</sub> .....   | 36 |
| Figure 16: <sup>13</sup> C NMR spectrum of 5-Nitro-1,10-Phenanthroline in CDCl <sub>3</sub> .....   | 37 |
| Figure 17: FTIR spectrum of 5-Nitro-1,10-Phenanthroline.....  | 38 |
| Figure 18: <sup>1</sup> H NMR spectrum of 5-Amine-1,10-Phenanthroline in DMSO .....   | 39 |
| Figure 19: Zoomed <sup>1</sup> H NMR spectrum of 5-Amine-1,10-Phenanthroline in DMSO .....  | 40 |
| Figure 20: <sup>13</sup> C NMR spectrum of 5-Amine-1,10-Phenanthroline in DMSO .....  | 41 |
| Figure 21: FTIR spectrum of 5-Amine-1,10-Phenanthroline .....   | 42 |
| Figure 22: <sup>1</sup> H NMR spectrum of tert-butyl 17-hydroxy-19,19-dimethyl- 3,6,9,12,15,18-hexaoxaicosanoate in CDCl <sub>3</sub> .....     | 43 |
| Figure 23: <sup>13</sup> C NMR spectrum of tert-butyl 17-hydroxy-19,19-dimethyl- 3,6,9,12,15,18-hexaoxaicosanoate in CDCl <sub>3</sub> .....    | 44 |
| Figure 24: FTIR spectrum of tert-butyl 17-hydroxy-19,19-dimethyl- 3,6,9,12,15,18-hexaoxaicosanoate .....  | 45 |
| Figure 25: GCMS chromatogram of tert-butyl 17-hydroxy-19,19-dimethyl- 3,6,9,12,15,18-hexaoxaicosanoate .....                                    | 46 |
| Figure 26: <sup>1</sup> H NMR spectrum of 2-hydroxy-1λ <sup>3</sup> ,4,7,10,13,16- hexaoxaoctadec- 1-yn-18-oic acid in CDCl <sub>3</sub> .....  | 47 |
| Figure 27: <sup>13</sup> C NMR spectrum of 2-hydroxy-1λ <sup>3</sup> ,4,7,10,13,16- hexaoxaoctadec- 1-yn-18-oic acid in CDCl <sub>3</sub> ..... | 48 |
| Figure 28: FTIR spectrum of 2-hydroxy-1λ <sup>3</sup> ,4,7,10,13,16- hexaoxaoctadec- 1-yn-18-oic acid ..  | 49 |
| Figure 29: HPLC chromatogram of 2-hydroxy-1λ <sup>3</sup> ,4,7,10,13,16- hexaoxaoctadec- 1-yn-18-oic acid.....                                  | 50 |
| Figure 30: FTIR spectrum of 2-chloro-1λ <sup>3</sup> ,4,7,10,13,16-hexaoxaoctadec-1-yn-18-oyl chloride..  | 51 |
| Figure 31: LC chromatogram of MSH(4)-PG .....   | 52 |
| Figure 32: Mass spectra of MSH(4)-PG .....  | 52 |
| Figure 33: HPLC chromatogram of MSH(4)-PG .....   | 53 |

## LIST OF SCHEMES

|   |    |
|---|----|
| Scheme 1: Reaction scheme for 5-amino-1,10-phenanthroline.....  | 8  |
| Scheme 2: Reaction scheme for the formation of lanthanide complexes.....                                | 9  |
| Scheme 3: Synthesis of the modified PEGO linker.....  | 10 |
| Scheme 4: Synthesis of 5-Nitro-1,10-Phenanthroline.....   | 14 |
| Scheme 5: Synthesis of 5-Amino-1,10-Phenanthroline.....   | 15 |
| Scheme 6: Synthesis of $\text{Eu}(\text{TТА})_3 \cdot 2\text{H}_2\text{O}$ .....                        | 16 |
| Scheme 7: Synthesis of 1,10-Phenanthroline- $\text{Eu}(\text{TТА})_3$ .....                             | 17 |
| Scheme 8: Synthesis of 5-Nitro-1,10-Phenanthroline- $\text{Eu}(\text{TТА})_3$ .....                     | 18 |
| Scheme 9: Synthesis of 5-Amino-1,10-Phenanthroline- $\text{Eu}(\text{TТА})_3$ .....                     | 19 |
| Scheme 10: Synthesis of tert-butyl 17-hydroxy-19,19- dimethyl-<br>3,6,9,12,15,18-hexaoxaicosanoate..... | 20 |
| Scheme 11: Synthesis of -hydroxy-1 $\lambda^3$ ,4,7,10,13,16-hexaoxaoctadec- 1-yn-18-oic acid.....      | 21 |
| Scheme 12: Synthesis of 2-chloro-1 $\lambda^3$ ,4,7,10,13,16-hexaoxaoctadec-1-yn-18-oyl chloride.....   | 22 |
| Scheme 13: Synthesis of 5-Amino-1,10-Phenanthroline.....  | 25 |
| Scheme 14: Synthesis of Luminescent Lanthanide Complexes.....   | 27 |
| Scheme 15: Synthesis of Polyethylene Glycol Linker.....   | 29 |

## LIST OF TABLES

|  |   |
|--|---|
| Table 1: Table of Melanocyte Stimulating Hormone Variations..... | 4 |
|--|---|



## ABSTRACT

### SYNTHESIS AND CHARACTERIZATION OF TIME-RESOLVED FLUORESCENCE PROBES FOR THE POTENTIAL DETECTION AND IMPROVED STUDY OF MELANOMA CANCER

Seth Alexander Sedberry

Western Carolina University (August, 2016)

Director: Dr. Carmen Huffman

A multi-part fluorescent probe was designed for the development of new clinical tools for the detection and treatment of melanoma skin cancer. It has been proposed that the addition of a fluorescent tag to a melanocyte stimulating hormone<sup>1</sup> would create a luminescent probe with potential for the detection and study of melanoma skin cancer. The proposed design involves attaching a luminescent lanthanide probe to an MSH (4) peptide substrate using a flexible polyethylene glycol linker. The individual portions of the proposed molecule (luminescent probe, PEGO linker, and MSH (4) peptide) have been synthesized and characterized using a combination of FTIR, NMR, GCMS, HPLC, UV-Vis, and Fluorescent spectroscopy.

Luminescent probe synthesis involved the nitration and subsequent reduction of 1,10-phenanthroline followed by complexation with  $\text{Eu}(\text{TTA})_3$ . Synthesis of the PEGO linker was accomplished by the reaction of tetraethylene glycol with tert-butyl bromoacetate to form a diacid through a t-butyl protected intermediate. MSH (4) peptide synthesis proceeded on solid phase following a f-moc protocol and using a Mars6 microwave synthesizer. Future work will focus on the construction of the final molecule using the components obtained herein.

## CHAPTER 1: INTRODUCTION

### 1.1 PROBLEM STATEMENT

Traditional forms of biological imaging suffer from various limitations that inhibit their use in medical applications. Limitations such as the presence of the background signal generated by the analyte's environment limit the sensitivity and dynamic range of the observation. Traditional chromophores make use of UV light to excite the luminophore, which damages the biological sample and is not ideal<sup>2</sup>. Other methods such as the use of chemical dyes exhibit photobleaching and poor chemical stability, which are disadvantageous. One way to overcome these obstacles is through the use of  $\text{Eu}^{3+}$  labels. Europium (III) luminophores are advantageous over traditional luminophores because of their long luminescent lifetimes and narrow emission bands, which in turn delivers greater assay sensitivity while also being capable of excitement in presence of visible light<sup>3</sup>. These properties make  $\text{Eu}^{3+}$  a prime target for use in the development of clinical tools for biological imaging.

### 1.2 BACKGROUND

#### 1.2.1 MALIGNANT MELANOMA AND G-PROTEIN COUPLED RECEPTORS

Cutaneous melanoma is a type of skin cancer that develops from pigment containing cells known as melanocytes, which in just 2012 occurred in 232,000 people and resulted in 55,000 deaths making it the most dangerous form of skin cancer<sup>4</sup>. The primary cause of melanoma skin cancer is exposure to UV light, generally from the sun or from tanning beds, which damages DNA in the skin. The damaged DNA emits a signal received by melanocytes, found between the dermal and epidermal layer of the skin, causing the production of melanin(**Fig. 1**).<sup>5</sup> Melanin has a direct positive effect because of its ability to absorb the energy from UV light and convert

it into heat. The earliest stage of melanoma begins with the uncontrolled, radial growth of the melanocytes<sup>6</sup>.

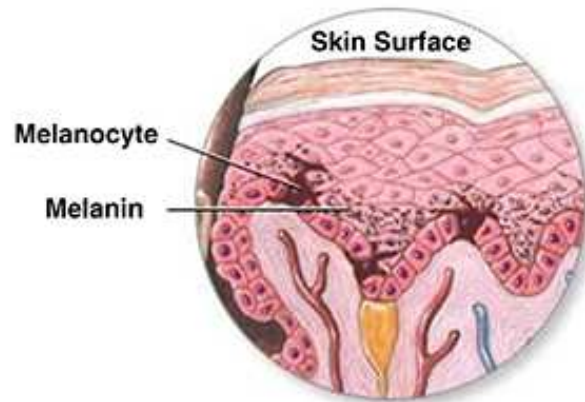


**Figure 1.** Location of melanocyte and melanin production in the skin<sup>5</sup>.

During this radial growth phase, the tumor remains less than 1mm thick and has not reached the blood vessels deeper in the skin, making it unlikely to spread throughout the body at that time<sup>6</sup>. If the tumor is detected during this phase, it can usually be completely removed with surgery. The development of melanoma is directly related to its ability to hijack the signaling mechanism that the body uses to protect skin DNA. Therefore the study of the signaling pathways of melanocytes is of high importance to the development of new clinical tools for detection and treatment of melanoma.

Melanocyte signaling pathways involve the activation and deactivation of G-Protein Coupled Receptors (GPCR's), which are the single largest family of cell-surface molecules involved in signal transmission and are present in just about every organ system.<sup>7</sup> The receptor is a globular polypeptide embedded in a cell's surface which binds to a signaling molecule, causing a conformational change and activating a G-Protein on the interior of the cell. In this

way GPCR's act like a switch, turning off or on through signal-receptor interactions on the cell's surface<sup>7,8</sup>. (Fig.2)

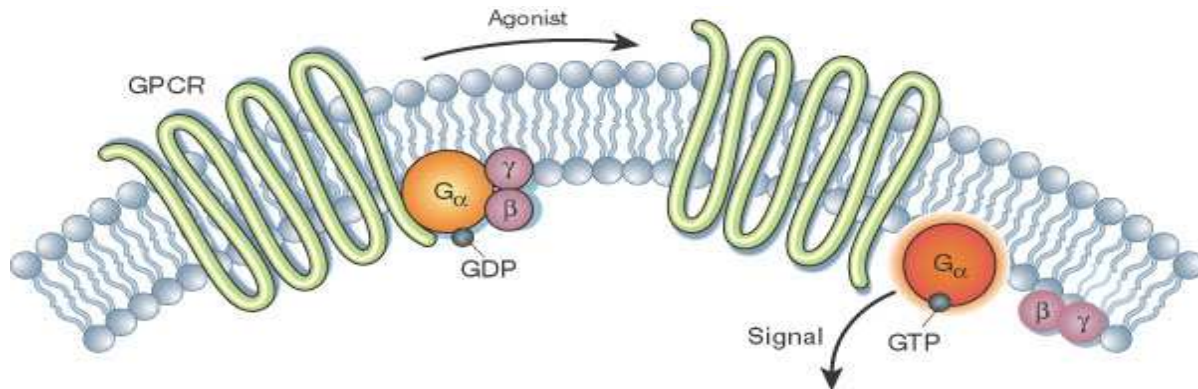


**Figure. 2.** A G-Protein Coupled Receptor activating a cell's signaling pathway through the presence of an agonist (signaling molecule)<sup>8</sup>.

This system is therefore regulated by the presence of a signaling molecule, which is in this instance a family of peptide hormones known collectively as melanocyte stimulating hormones (MSH). This family consists of an alpha, a beta, and a gamma hormone which are produced by cells in the intermediate lobe of the pituitary gland<sup>1</sup>. These short peptides all share the conserved **His-Phe-Arg-Trp** amino acid sequence (Table 1).

|                                 |  |
|---------------------------------|--|
| <b><math>\alpha</math>-MSH:</b> | Ac-Ser-Tyr-Ser-Met-Glu- <b>His-Phe-Arg-Trp</b> -Gly-Lys-Pro-Val                                  |
| $\beta$ -MSH (human):           | Ala-Glu-Lys-Lys-Asp-Glu-Gly-Pro-Tyr-Arg-Met-Glu- <b>His-Phe-Arg-Trp</b> -Gly-Ser-Pro-Pro-Lys-Asp |
| $\beta$ -MSH (porcine):         | Asp-Glu-Gly-Pro-Tyr-Lys-Met-Glu- <b>His-Phe-Arg-Trp</b> -Gly-Ser-Pro-Pro-Lys-Asp                 |
| $\gamma$ -MSH:                  | Tyr-Val-Met-Gly- <b>His-Phe-Arg-Trp</b> -Asp-Arg-Phe-Gly   |

**Table 1.** Table of Melanocyte Stimulating Hormone Variations

These hormones (primarily  $\alpha$ -MSH) bind with GPCR's to signal the production of melanin in the skin. Because of this ability to bind with the cell surface of the melanocyte, MSH peptides are good targets for the development of clinical tools for the imaging, detection, and study of melanoma skin cancer<sup>1</sup>. We have proposed that using a MSH peptide as a foundation, a luminescent lanthanide complex could be tethered to the hormone using a polyethylene glycol linker in an attempt to make a biologically active fluorescent tag for the study of the melanocyte signaling pathway.

### 1.2.2 LANTHANIDE AND LIGAND CHEMISTRY

Lanthanide complexes exhibit properties such as having narrow emission bands and a long luminescent lifetime. These properties make them favorable candidates for possible bio-imaging agents. The lanthanide (III) ion's narrow emission bands are due to the shielding of the

4f orbitals by the filled 5s and 5p sub-shells.<sup>9</sup> However direct excitation of f-electrons from lanthanide (III) is difficult. This is because of the forbidden nature of 4f-4f electronic transitions due to their orbital parity being the same in both the initial and final states (Laporte forbidden).<sup>10</sup> Selection rules dictate that excitation of the lanthanide (III) ion must occur during a temporary change in geometric arrangement around the ion or mixing with opposite parity wave functions from 5d orbitals, ligand orbitals, or charge transfer states<sup>3</sup>. Because of the low probability of an electric dipole f-f transition and direct excitation of the lanthanide is difficult. As a result an organic chromophore ligand is required to transfer energy to the lanthanide (III) ion and induce luminescence. The organic ligand forms a chelate with the lanthanide and transfers absorbed energy to the luminophore through a process described as “the antenna effect” (Fig. 3).<sup>3</sup>

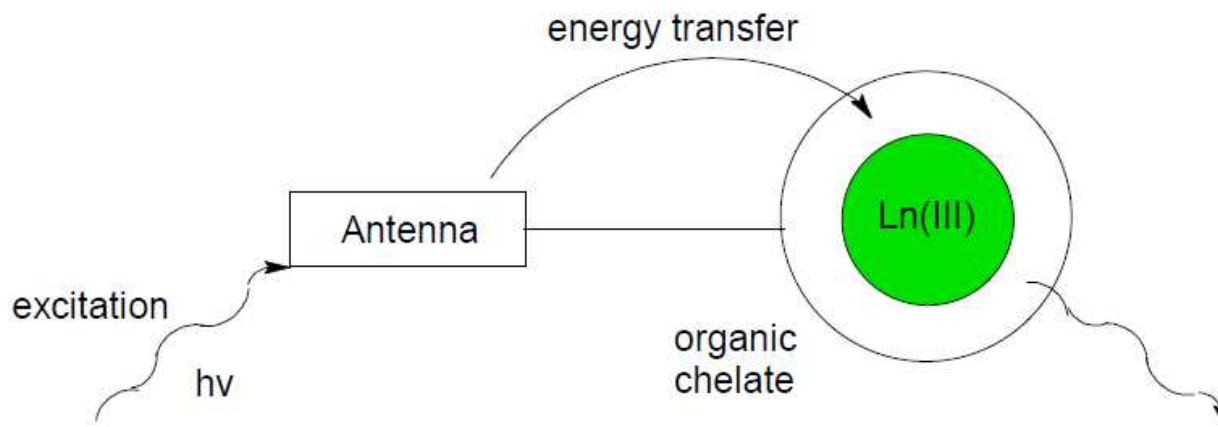


**Figure 3.** The “Antenna Effect”<sup>2</sup>

Through intersystem crossing, the excited electrons inhabit the triplet state of the ligand and can then transfer energy from the triplet state to the emissive state of the lanthanide complex center<sup>9</sup>. To maximize efficiency, the antenna ligand needs to have a triplet state ( $T_1$ ) energy that is close to the energy of the lanthanide (III) ion to achieve the energy transfer necessary for emission<sup>10</sup>.

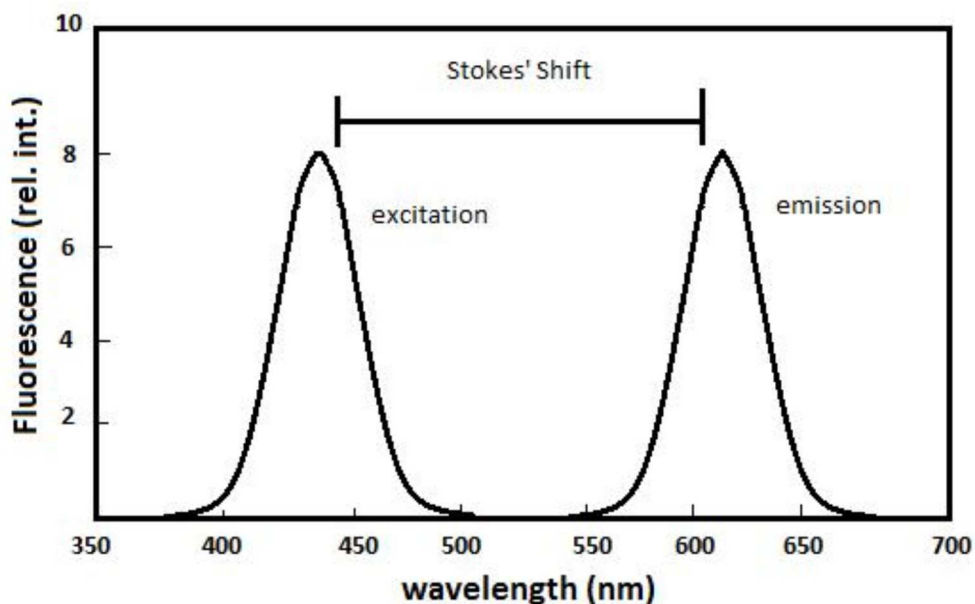


**Figure 4.** Visualization of a Stoke's Shift<sup>12</sup>

Europium (III) complexes are specifically advantageous over other lanthanide complexes because they can be sensitized with visible, longer wavelength light as opposed to shorter wavelength UV excitation and is less harmful to biological targets, which is a primary objective in the development of clinical tools. Additional advantages of Europium complexes include a narrow emission line in the red light region and a long luminescent lifetime which guarantees minimal interference from fluorescing biological samples<sup>11</sup>. This as well as a large Stokes shift and a high quantum yield make  $\text{Eu}^{3+}$  a prime target for coordination with organic chromophore ligands used in biological imaging applications 2,<sup>12</sup>. **(Fig. 4)**

### 1.3 OBJECTIVES

The proposed molecule can be split up into three distinct components: a fluorescent lanthanide complex, a polyethylene glycol linker, and a melanocyte stimulating hormone (MSH (4)). **(Fig. 5)**

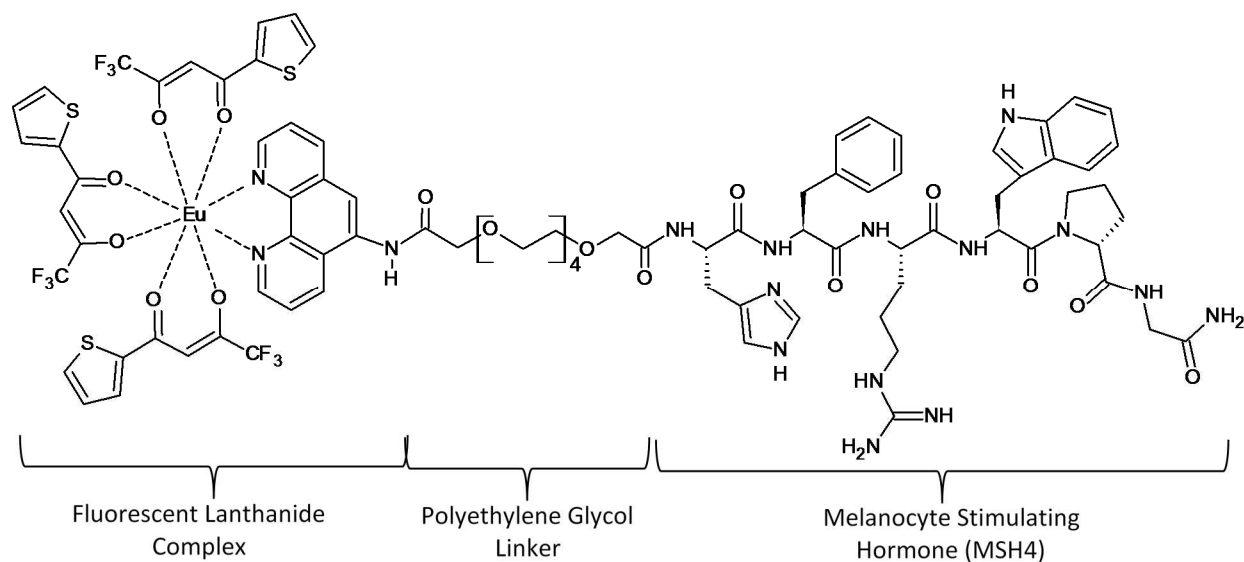


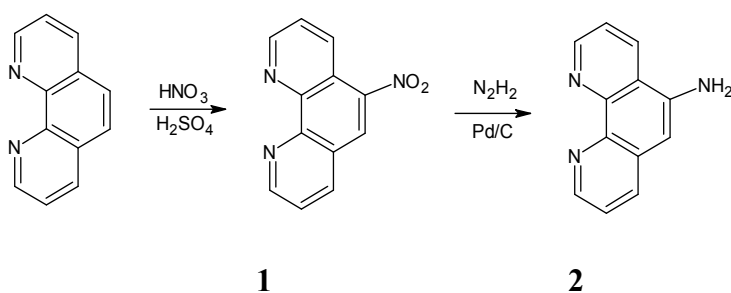
**Figure 5.** Three component design of the proposed molecule.

The melanocyte stimulating hormone is a peptide produced by the pituitary gland and functions to bind with the G-protein coupled receptor found in the cell membrane of the melanocyte that is up-regulated in melanoma cancer cells. Attached to the MSH (4)-PG peptide (10) is a luminescent lanthanide complex (6). This lanthanide chelate tag is composed of a phenanthroline chromophore (2) which acts to absorb light and transfer it to the lanthanide metal, the emission of which can be used to detect the molecule. Tethering the peptide and lanthanide chelate is a polyethylene glycol linker (8) that both tethers the two together while ensuring that the two remain far enough apart to allow for proper binding of the peptide at the melanocyte's g-protein coupled receptors. Goals of this research project include: synthesis of an organic phenanthroline chromophore (2), synthesis of a polyethylene glycol linker (8), synthesis of a melanocyte stimulating hormone peptide (10), final assembly of the three previously listed components on a solid phase resin, cleavage from the solid phase resin, and final formation of the luminescent lanthanide complex. The completed molecule should then be able to function as



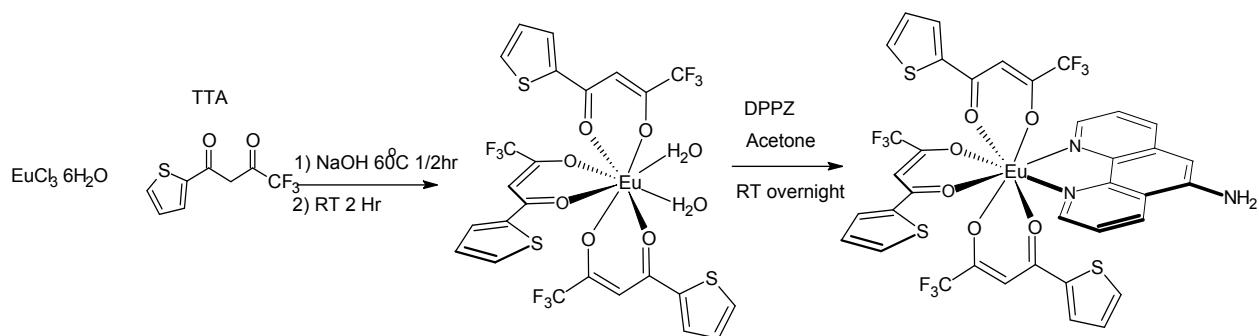
a biologically active luminescent tag with the potential for use as a clinical tool to detect and study melanoma skin cancer.

Synthesis of an organic phenanthroline chromophore was first achieved. The 5-Amino-1,10-phenanthroline (**2**) was synthesized from 1,10-phenanthroline through a nitration reaction followed by a reduction of the attached nitro group<sup>12</sup> (**Scheme 1**). Firstly fuming nitric acid was added to a refluxing solution of 1,10-phenanthroline in sulfuric acid to yield 5-nitro-1,10-phenanthroline (**1**). 5-Nitro-1,10-phenanthroline (**1**) was then reduced to 5-amino-1,10-phenanthroline (**2**) using hydrazine and a palladium catalyst to form a ligand with an amine functional group for the attachment of the PEGO linker. These compounds were characterized by FT-IR, GCMS, and NMR.



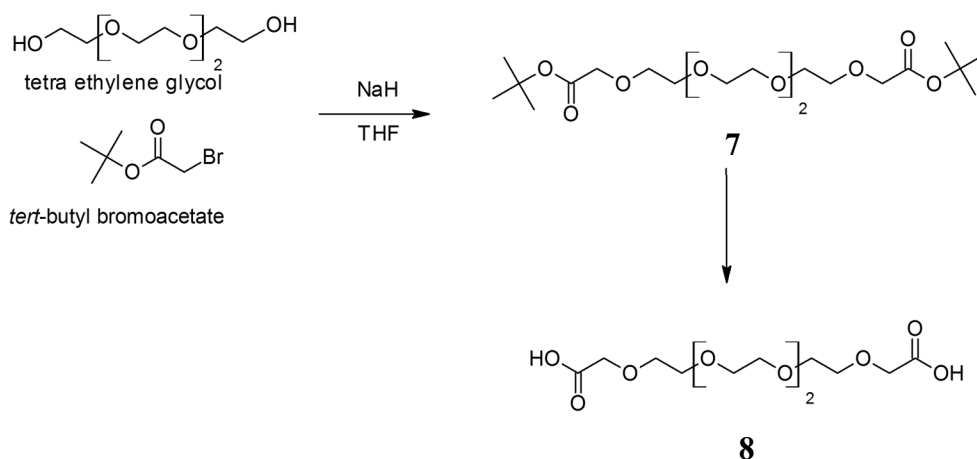
**Scheme 1.** The synthesis of 5-Amino-1,10-Phenanthroline involves the reduction of 5-Nitro-1,10-Phenanthroline from the nitrated 1,10-Phenanthroline in 64% and 84% yield respectively.

The three ligands were then complexed with a previously synthesized  $\text{Eu}(\text{TTA})_3 \cdot 2\text{H}_2\text{O}$  (**3**) molecule to form functional luminescent molecules, which were characterized using a combination of UV-Vis and fluorescent spectroscopy to form a qualitative luminescent profile of the molecules (**Scheme 2**). Analysis revealed an absorbance max of  $\sim 340$  nm and a strong emission at  $\sim 615$  nm.



**Scheme 2.** Complexation involves the reaction of  $\text{EuCl}_3 \cdot 6\text{H}_2\text{O}$  with TTA to form  $\text{Eu}(\text{TTA})_3 \cdot 2\text{H}_2\text{O}$  in 31% yield. This was reacted with a phenanthroline ligand to form a luminescent tag.

To achieve attachment of the luminescent tag with the binding peptide, a linker must be used that fulfills two requirements: it must remain soluble while also maintaining enough distance between to allow the peptide to allow proper binding to the receptor. Accordingly, a modified polyethylene glycol diacid (**8**) was chosen for the proposed linker due to its ability to bond with amine groups while maintaining solubility. Linker synthesis was accomplished by combining tetraethylene glycol and tert-butyl bromoacetate in a solution of sodium hydride and THF.<sup>13</sup> The resulting t-butyl protected PEGO (**7**) structure was next reacted in formic acid to yield the deprotected PEGO (**8**) structure capable of replicating the C-terminus end of a peptide structure rendering it able to couple with amines (**Scheme 3**).<sup>14</sup> Compounds were analyzed using a combination FT-IR, GCMS, HPLC and NMR to confirm successful synthesis.



**Scheme 3.** Synthesis of the modified PEGO (**7**) linker involves the nucleophilic addition of tert-butyl bromoacetate to tetra ethylene glycol occurred in 82% yield. Deprotection with formic acid produced the deprotected PEG linker **8** in quantitative yield. This molecule will attach the luminescent tag to the binding peptide.

The third portion of synthesis regarded the microwave assisted solid phase synthesis of the MSH (4)-PG peptide (**10**). The MSH (4) peptide was chosen for its ability to bind with melanocyte surface receptors. A proline-glycine residue was added to the peptide to increase distance between the ligand and the binding site in an effort to increase affinity. The peptide was synthesized on a rink amide resin with assistance from a Mars6 microwave synthesizer. Completed peptide was analyzed using LCMS and HPLC to reveal purity of greater than 90% at the target mass.

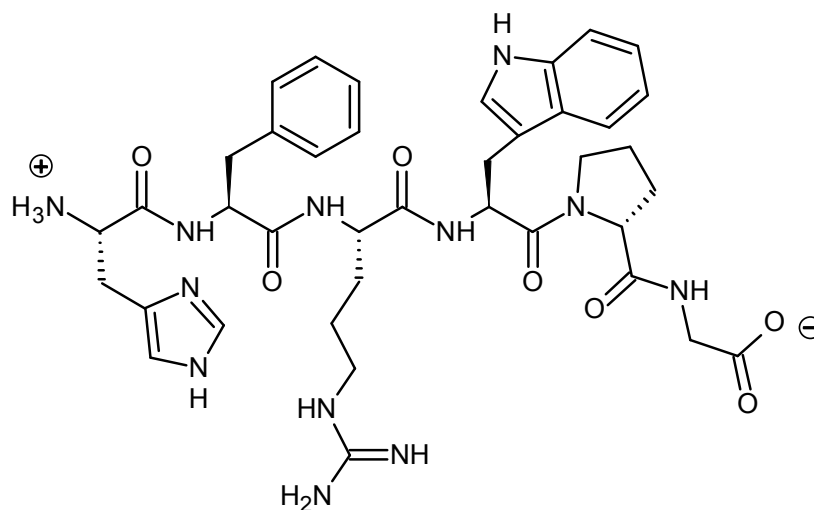


**Figure 6.** MSH (4) –PG (His-Phe-Arg-Trp-Pro-Gly)

This research concluded with an attempt to complete the final molecule. The reaction protocol attempted to first attach one terminus of the PEGO linker to the phenanthroline ligand, with the second terminus remaining a carboxylic acid. This was proposed in an effort to prevent cross coupling of the PEGO linker with the peptide substrate. The reaction protocol next called for the attachment of the newly formed linker-ligand molecule to the peptide on solid phase to form the proposed peptide-linker-ligand compound. Once obtained, this molecule could then be cleaved from the resin and mixed in solution with  $\text{Eu}(\text{TTA})_3 \cdot 2\text{H}_2\text{O}$  to form a luminescent chelate-completing synthesis of the target molecule.

## CHAPTER 2: EXPERIMENTAL

All reagents were purchased from Sigma Aldrich or Acros Organics and used without further purification unless otherwise stated. Synthesized ligands and complexes were characterized using Fourier-transform infrared spectroscopy (FT-IR), nuclear magnetic resonance (NMR, when applicable), UV-visible and fluorescence spectroscopic techniques, high pressure liquid chromatography (HPLC), gas chromatography (GC), and mass spectroscopy (GCMS, LCMS). The methods used for characterization will be discussed in this section along with all instrument specifications.

### 2.1 MATERIALS AND INSTRUMENTATION

#### 2.1.1 FTIR

FT-IR spectra were obtained using a Perkin Elmer Spectrum One. All measurements were performed at room temperature with a scanning range of  $4000\text{ cm}^{-1}$  –  $600\text{ cm}^{-1}$ , using single-bounce attenuated total reflectance with a diamond crystal. For all of the materials that were measured as a solid powder (all solvents had been removed), the background was performed on the instrument room environment. The ATR plate was cleaned with a Kimwipe and acetone between each measurement.

#### 2.1.2 NUCLEAR MAGNETIC RESONANCE SPECTROSCOPY (NMR)

NMR spectra were obtained using a JEOL 300 MHz Eclipse NMR with a 5 mm probe capable of detecting  $^1\text{H}$  and  $^{13}\text{C}$  nuclei. Proton NMR samples were prepared using ~10 mg of material, in either deuterated chloroform ( $\text{CDCl}_3$ ) or deuterated dimethyl sulfoxide ( $\text{d}_6\text{-DMSO}$ ) unless otherwise stated, and spectra were obtained using a varying number of scans ranging from 16-128 as to ensure an adequate signal-to-noise ratio was acquired.  $^{13}\text{C}$  NMR samples were

prepared similarly, except material was added until the deuterated solution became saturated.

### 2.1.3 UV-VISIBLE ABSORPTION SPECTROSCOPY

UV-Vis spectra were collected using an Agilent 8453 UV-Vis spectrometer at room temperature. This instrument has two different sources: a deuterium lamp (for UV measurements), and a tungsten lamp (for visible measurements). The use of a photodiode array detector allows the spectrometer to detect a wavelength range of 190 nm – 1100 nm at 1 nm intervals. All of the blank and sample measurements were made using a quartz cuvette (1 cm path length).

### 2.1.4 FLUORESCENCE SPECTROSCOPY

Fluorescence spectra were acquired using a Perkin Elmer LS-55 Luminescence Spectrometer at room temperature. The same solvent systems for the blanks (to correct for any solvent fluorescence), samples and references that were used for UV-Vis measurements were also used for fluorescence measurements. A quartz cuvette was used for all measurements. A scanning range of 200 nm – 800 nm with a scan speed of 200 nm/min was used, with an excitation and emission slit of 5.0 nm. Detection was accomplished a delay time of up to 400  $\mu$ s following 340 nm excitation.

### 2.1.5 GAS CHROMATOGRAPHY

Gas chromatograms were obtained using an Agilent Technologies 7890 A GC System with a 7693 Autosampler, a 5975 C Inert XL EI/CI MSD (with Triple Axis Detector), and an Agilent J&W GC Column-HP-5MS (30 m  $\times$  0.25 mm  $\times$  0.25  $\mu$ m) using a split inlet. Flow rate: 1.2mL/min, APC-3 pressure: 1.0, Inlet Temperature: 250°C, Oven Temperature: 80°C, MS Quad Temperature: 150°C, MS Source Temperature: 230°C.

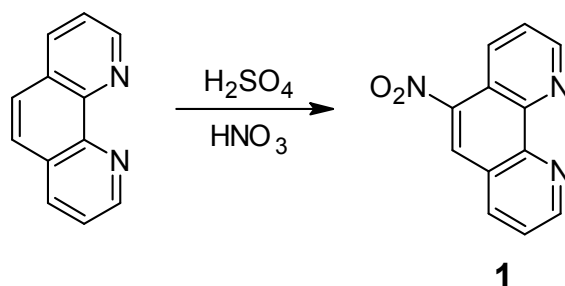
### 2.1.6 LIQUID CHROMATOGRAPHY

High pressure liquid chromatography was performed using an Agilent Technologies 1220 Infinity LC with a 99301 Prevail Select C18 column (L: 250 mm, ID: 4.6 mm) and a UV-Vis

detector. Mobile phase: A: 10% CH<sub>3</sub>CN B: 90% H<sub>2</sub>O, Flow Rate: 1.5mL/min, Column Temperature: 25°C, Detection: 214nm/280nm. LCMS was performed off site.

## 2.2 FUNCTIONALIZED PHENANTHROLINE LIGAND AND EU<sup>3+</sup> COMPLEX SYNTHESIS

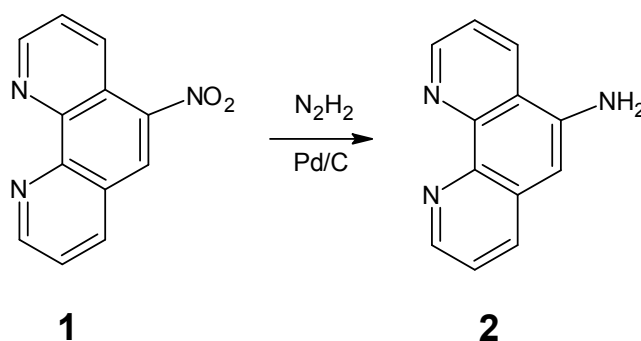
### 2.2.1 SYNTHESIS OF 5-NITRO-1,10-PHENANTHROLINE



**Scheme 4.** Synthesis of 5-Nitro-1, 10-Phenanthroline

*5-Nitro-1,10-Phenanthroline (1).* 1,10-phenanthroline (2.5g, 12.611 mmol, 1.0 eqv) was dissolved in Sulfuric acid (7.5 ml, 0.473 mol, 37.5 eqv) and heated to 160° C while stirring. Nitric acid (15 ml, 0.189 mol, 15 eqv) was added drop wise to the mixture and the resulting solution was stirred at 160 ° C for 3 hours. Upon addition of HNO<sub>3</sub> the reaction violently evolved brown gas and refluxed. The resulting clear-orange solution was then brought to room temperature and adjusted to a pH of 3 with a 3M solution of NaOH. The yellow solid precipitant was then filtered and dried to yield 5-nitro-1,10-phenanthroline (**1**) (1.805 g, 8.015 mmol, 63.5 % yield). m.p. = 217-220 °C. NMR(300MHz, CDCl<sub>3</sub>) δ 9.25 (2H, mult.), δ 8.935(1H, dd, J = 3 Hz,9 Hz), δ 8.60 (1H, s), δ 8.360(1H, dd, J = 3 Hz, 9Hz), δ 7.74(2H, mult.). <sup>13</sup>C NMR (300 MHz, CDCl<sub>3</sub>) δ = 153.4, 151.4, 147.5, 146.0, 144.1, 137.7, 132.3, 125.4, 125.3, 124.3, 124.2, 120.8 ppm. FTIR (ATR): 1516, 1503, 1344, 831, 804, 731 cm<sup>-1</sup>.

## 2.2.2 SYNTHESIS OF 5-AMINO-1,10-PHENANTHROLINE

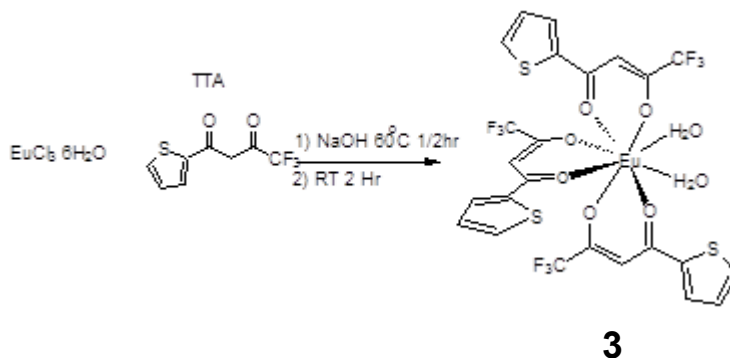


**Scheme 5.** Synthesis of 5-Amine-1, 10-Phenanthroline

*5-Amino-1,10-Phenanthroline (2).* 5-Nitro-1,10-phenanthroline (**1**) (1.805g, 8.105 mmol, 1 eqv) was reacted in ethanol (30 ml) with hydrazine monohydrate (4.64 ml, 0.143 mol, 17.5 eqv) and a palladium on carbon catalyst (300 mg). 5-Nitro-1,10-phenanthroline (**1**) was first dissolved in ethanol, the palladium catalyst was added, and the solution was purged with argon. Hydrazine monohydrate was then added drop-wise over 30 minutes via syringe and the reaction mixture was heated to 70°C for 10 hours. The reaction gained a bronze tint as it lightly refluxed. The reaction mixture was then filtered and the solvent was removed under vacuum to yield 5-amino-1,10-phenanthroline (**2**) (1.318g, 6.75 mmol, 84.3%) as a dry, bright red solid. m.p. = 140-143°C NMR (300 MHz, DMSO)  $\delta$  9.06 (1H, d, J = 3Hz),  $\delta$  8.71 (2H, dd, J = 3 Hz, 9 Hz),  $\delta$  8.16 (1H, d, J = 9 Hz),  $\delta$  7.79 (1H, mult.),  $\delta$  7.58 (1H, mult.),  $\delta$  6.89 (1H, s). <sup>13</sup>C NMR  $\delta$  = 153.43, 151.35, 137.74, 132.31, 125.38, 124.29, 124.20, 120.83, 77.42, 77.00, 76.57. FTIR (ATR): 3423, 3363, 3221, 1638, 1587, 1377, 1291, 1046, 867, 786, 734, 656 cm<sup>-1</sup>.



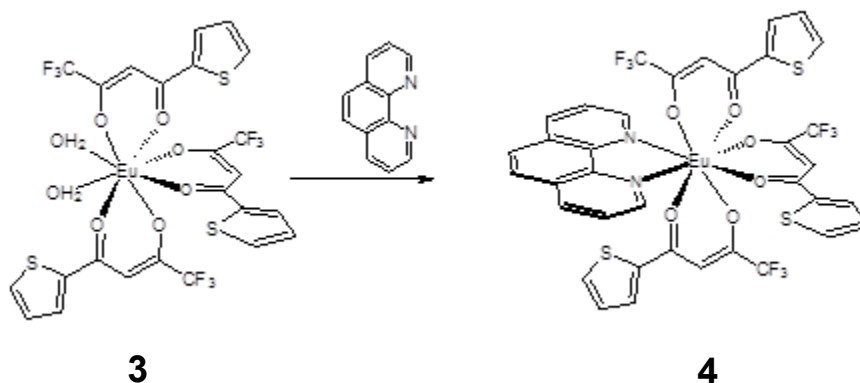
### 2.2.3 SYNTHESIS OF $\text{Eu}(\text{TTA})_3 \cdot 2\text{H}_2\text{O}$



**Scheme 6.** Synthesis of  $\text{Eu}(\text{TTA})_3 \cdot 2\text{H}_2\text{O}$

$\text{Eu}(\text{TTA})_3 \cdot 2\text{H}_2\text{O}$  (**3**) Europium chloride hexahydrate (0.2582 g, 1 mmol, 1 eqv) was dissolved in 10ml de-ionized  $\text{H}_2\text{O}$ . In a second flask, NaOH (0.118 g, 3 mmol, 3 eqv) and theonyltrifluoroacetone (0.999 g, 4.5 mmol, 4.5 eqv) was dissolved in 10ml de-ionized  $\text{H}_2\text{O}$  at  $40^\circ\text{C}$ . The second solution of NaOH and TTA was then added drop wise to the first solution of europium chloride hexahydrate while stirring. The combined solution was stirred at  $50^\circ\text{C}$ - $55^\circ\text{C}$  for 0.5 hours then stirred at room temperature for 2.5 hours. The reaction solution was filtered to obtain a white precipitant which was then washed with 500ml de-ionized  $\text{H}_2\text{O}$  and 3ml hexane to yield  $\text{Eu}(\text{TTA})_3 \cdot 2\text{H}_2\text{O}$  (**3**) (0.267 g, 0.312mmol, 31.2%).

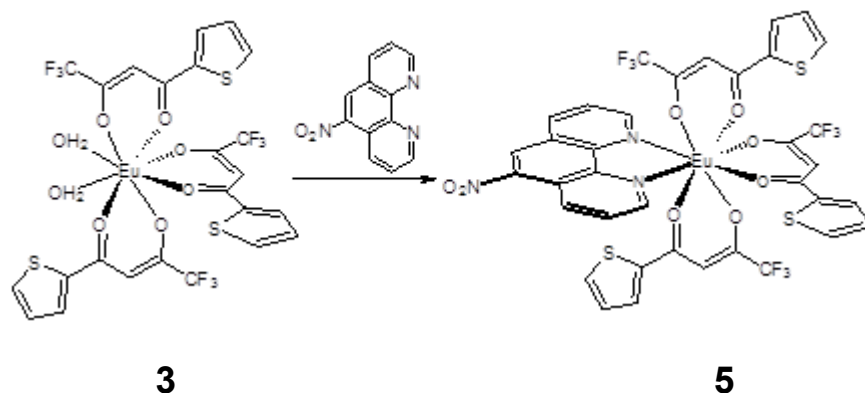
## 2.2.4 SYNTHESIS OF 1,10-PHENANTHROLINE-EU(TTA)<sub>3</sub> COMPLEX



**Scheme 7.** Synthesis of 1,10-Phenanthroline - Eu(TTA)<sub>3</sub>

*1,10-Phenanthroline - Eu(TTA)<sub>3</sub> (4)*. 1,10-phenanthroline (13.8mg, 0.07mmol, 1 eqv.) was dissolved in 10ml of methanol and stirred. In a separate Erlenmeyer flask, Eu(TTA)<sub>3</sub>·2H<sub>2</sub>O (**3**) (60mg, 0.07mmol, 1 eqv.) was dissolved in 5ml CHCl<sub>3</sub>. The Europium solution was then added drop wise to the stirring phenanthroline solution. Afterward the reaction was stirred at room temperature for 24 hours and filtered to yield 1,10-phenanthroline - Eu(TTA)<sub>3</sub> (**4**) as a white precipitant. Product characterized via Uv-Vis and fluorescent spectroscopy.

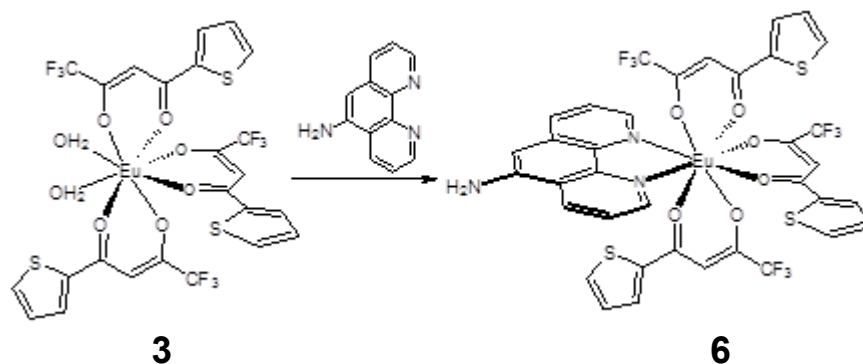
## 2.2.5 SYNTHESIS OF 5-NITRO-1,10-PHENANTHROLINE-EU(TTA)<sub>3</sub> COMPLEX



**Scheme 8.** Synthesis of 5-Nitro-1,10-Phenanthroline - Eu(TTA)<sub>3</sub>

*5-Nitro-1,10-Phenanthroline - Eu(TTA)<sub>3</sub> (5).* 5-Nitro-1,10-phenanthroline (**1**) (11.87 mg, 0.07 mmol, 1 eqv.) was dissolved in 10ml of methanol and stirred. In a separate Erlenmeyer flask, Eu(TTA)<sub>3</sub>·2H<sub>2</sub>O(**3**) (60 mg, 0.07 mmol, 1.3 eqv.) was dissolved in 5ml CHCl<sub>3</sub>. The Europium solution was then added drop wise to the stirring phenanthroline solution. Afterward the reaction was stirred at room temperature for 24 hours and filtered to yield 5-nitro-1,10-phenanthroline - Eu(TTA)<sub>3</sub> (**5**) as a yellow precipitant. Product characterized via Uv-Vis and fluorescent spectroscopy.

## 2.2.6 SYNTHESIS OF 5-AMINO-1,10-PHENANTHROLINE-EU(TTA)<sub>3</sub> COMPLEX

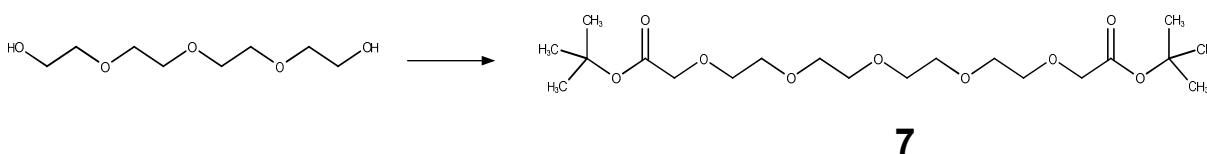


**Scheme 9.** Synthesis of 5-Amine-1,10-Phenanthroline-Eu(TTA)<sub>3</sub>

*5-Amino-1,10-Phenanthroline - Eu(TTA)<sub>3</sub> (6).* 5-amino-1,10-phenanthroline (**2**) (13.7 mg, 0.07 mmol, 1 eqv.) was dissolved in 10ml of methanol and stirred. In a separate Erlenmeyer flask, Eu(TTA)<sub>3</sub>-2H<sub>2</sub>O (**3**) (60 mg, 0.07 mmol, 1 eqv.) was dissolved in 5ml CHCl<sub>3</sub>. The Europium solution was then added drop wise to the stirring phenanthroline solution. Afterward the reaction was stirred at room temperature for 24 hours and filtered to yield 5-amino-1,10-phenanthroline-Eu(TTA)<sub>3</sub> (**5**) as an orange precipitant. Product characterized via Uv-Vis and fluorescent spectroscopy.

## 2.3 POLYETHYLENE GLYCOL LINKER SYNTHESIS

### 2.3.1 SYNTHESIS OF TERT-BUTYL 17-HYDROXY-19,19-DIMETHYL-3,6,9,12,15,18-HEXAOXAIOSANOATE



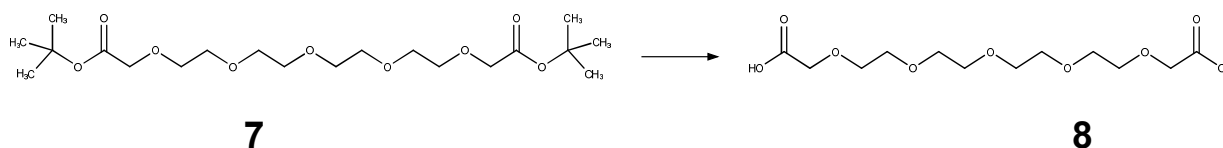
**Scheme 10.** Synthesis of tert-butyl 17-hydroxy-19,19-dimethyl-3,6,9,12,15,18-hexaoxaicosanoate

*Tert-butyl 17-hydroxy-19,19-dimethyl-3,6,9,12,15,18-hexaoxaicosanoate (7).* Tetraethylene glycol (1.0 g, 0.89 ml, 5.14mmol, 1.0 eqv) was added slowly to a stirred solution of sodium hydride in 10ml of dry THF and stirred at room temperature for 2 hours. Following this, Tert-butyl bromoacetate (3.0 g, 2.28ml, 15.44mmol, 3 eqv) was dissolved in a separate 10ml solution of dry THF and the glycol solution was chilled in an ice bath. The tert-butyl bromoacetate solution was then added drop wise to the chilled glycol solution. The reaction was stirred at 0°C for 2 hours, then at room temperature for 10 hours. Solvent was then removed under rotary evaporation; the remaining residue was dissolved with water and extracted with diethyl ether. The extract was dried over magnesium sulfate and the solvent was removed under rotary evaporation. The remaining residue was then heated and stirred under vacuum to remove remaining starting material yielding tert-butyl 17-hydroxy-19,19-dimethyl-3,6,9,12,15,18-hexaoxaicosanoate (**7**) as a viscous clear yellow oil (1.779 g, 4.204mmol, 81.79% yield). GCMS analysis revealed that the sample was 93% pure as demonstrated by area under the curve. NMR (300 MHz, CDCl<sub>3</sub>) δ 3.94 (4H, s), δ 3.60 (16H), δ 1.40 (18H, s). C<sub>13</sub> NMR (300 MHz, CDCl<sub>3</sub>)

$\delta = 169.46, 81.25, 77.43, 77.00, 70.48, 70.36, 68.79, 27.88.$

FTIR (ATR): 2979, 2870, 1747, 1366, 1224, 1120, 945, 844, 746  $\text{cm}^{-1}$ . GC/MS: m/z:  $[\text{M}^+]$  265.1, 147, 103, 57 -  $\text{C}(\text{CH}_3)_3$ , 41.

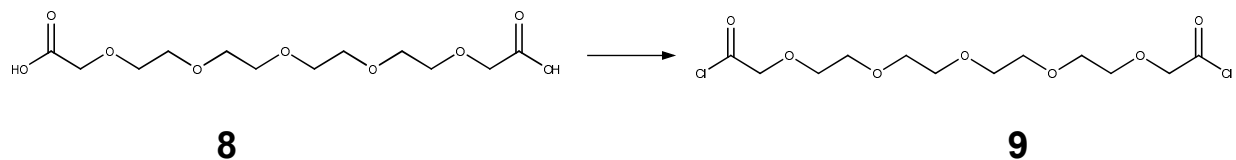
### 2.3.2 SYNTHESIS OF 2-HYDROXY-1 $\lambda^3$ ,4,7,10,13,16-HEXAOXAOCTADEC-1-YN-18-OIC ACID



**Scheme 11.** Synthesis of -hydroxy-1 $\lambda^3$ ,4,7,10,13,16-hexaoxaoctadec- 1-yn-18-oic acid

*2-hydroxy-1 $\lambda^3$ ,4,7,10,13,16-hexaoxaoctadec-1-yn-18-oic acid (8)*. Tert-butyl 17-hydroxy-19,19-dimethyl-3,6,9,12,15,18-hexaoxaicosanoate (**7**) (1 eqv) was dissolved in 5ml of formic acid and stirred at room temperature for 2 hours. Solvent was then removed under rotary evaporation to yield 2-hydroxy-1 $\lambda^3$ ,4,7,10,13,16-hexaoxaoctadec- 1-yn-18-oic acid (**8**) as a clear-yellow fluid oil (1.293g, 4.169mmol, 99% yield). HPLC analysis revealed a purity of 92% as demonstrated by area under the curve. NMR (300 MHz,  $\text{CDCl}_3$ )  $\delta$  10.24 (2H, s),  $\delta$  4.16 (4H, s),  $\delta$  3.70 (16H, multi.)  $\text{C}_{13}$  NMR (300 MHz,  $\text{CDCl}_3$ )  $\delta = 173.93, 77.60, 77.18, 76.76, 71.21, 70.61, 70.37, 68.69.$  FTIR (ATR): 2921, 2874, 1728, 1421, 1348, 1196, 1088, 946, 846, 670  $\text{cm}^{-1}$ .

### 2.3.3 SYNTHESIS OF 2-CHLORO-1 $\lambda^3$ ,4,7,10,13,16-HEXAOXAOCTADEC-1-YN-18-OYL CHLORIDE



**Scheme 12.** Synthesis of 2-chloro-1 $\lambda^3$ ,4,7,10,13,16-hexaoxaoctadec-1-yn-18-oyl chloride

*2-chloro-1 $\lambda^3$ ,4,7,10,13,16-hexaoxaoctadec-1-yn-18-oyl chloride (9)*. 2-hydroxy-1 $\lambda^3$ ,4,7,10,13,16-hexaoxaoctadec-1-yn-18-oic acid (**8**) (1 eqv) and oxalyl chloride (4 eqv) were mixed in 80ml of benzene in a round bottom flask under argon and stirred at room temperature. To the mixture, 4 drops of DMF was added and the reaction mixture was stirred at room temperature for 6 hours. Oxalyl chloride and benzene were then removed under rotary evaporation to yield 2-chloro-1 $\lambda^3$ ,4,7,10,13,16-hexaoxaoctadec-1-yn-18-oyl chloride(**9**) as a brown resin. The obtained product was verified on FT-IR and was used for subsequent synthesis without purification. FTIR (ATR): 3125, 2921, 2874, 1806, 1454, 1408, 1356, 1119, 928, 742, 678  $\text{cm}^{-1}$ .

## 2.4 PEPTIDE SYNTHESIS

### 2.4.1 SYNTHESIS OF MELANOCYTE STIMULATING HORMONE (4) - PG

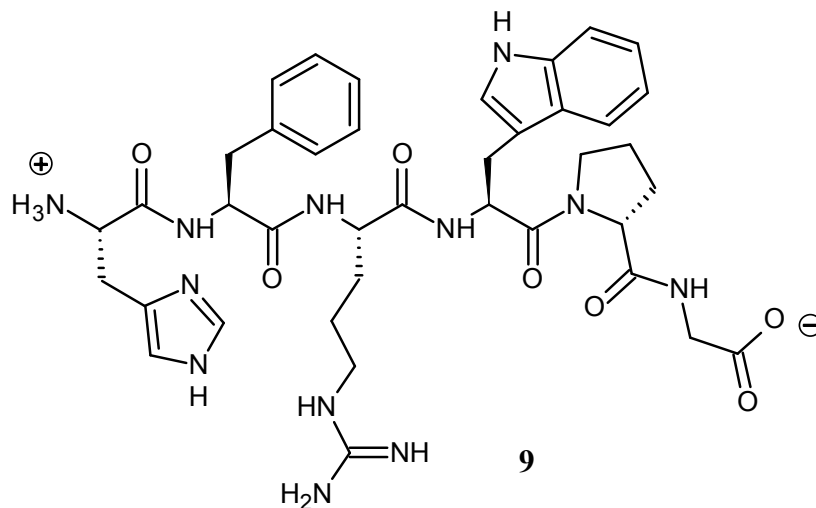


**Figure 7.** Melanocyte Stimulating Hormone (4) -PG (His-Phe-Arg-Trp-Pro-Gly) (**9**)

*Melanocyte Stimulating Hormone(4)-PG (9)*. Synthesis was performed on solid support in a Mars6 microwave synthesizer with fiber optic temperature sensor from CEM Corp.

Approximately 1250mg (0.5mmol) of Fmoc-Gly-CLEAR-Amide Resin was placed in a 50mL fritted plastic reaction vessel and the resin was swelled in 50% DMF and 50% DCM for one hour. The initial deprotection was performed with about 6mL of 20% piperidine in DMF for 30 seconds at 70°C followed by 30 seconds at 75°C. The resin was washed with DMF and a Kaiser test performed to confirm the presence of a primary amine. A 3-fold excess of the first amino acid was dissolved in DMF along with a 5-fold excess of Oxyma pure (coupling reagent). A 5-fold excess of DIC was added to the amino acid mixture and then the entire volume was added to the resin. Coupling was performed for five minutes at 75°C. Another Kaiser test was then performed to confirm completion of the coupling reaction. The deprotection and coupling cycle



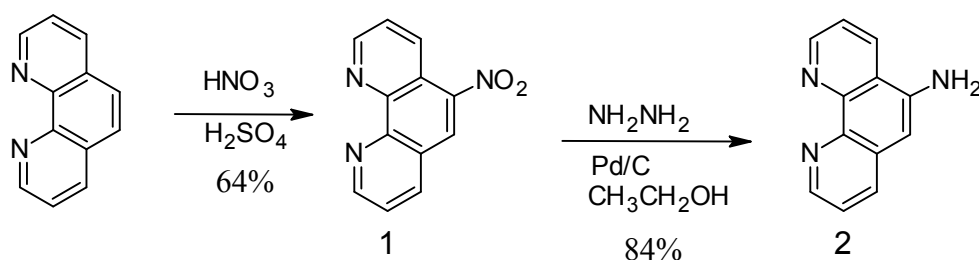
was repeated as necessary until all amino acids were added to the growing peptide chain. After addition of the last amino acid the resin was washed with DCM, and stored at 4°C. Due to the metal interior of the Mars6 microwave, cleavage of the peptide chain was performed on bench top. Approximately 6ml of cleavage cocktail (90% TFA/3% H<sub>2</sub>O/3% 1,2-ethanedithiole/3% thioanisole) was added to the dried resin and cleavage was performed at room temperature for 6 hours. Cleaved peptide was collected by filtration, precipitated in cold ether, and centrifuged for 30 minutes at 4°C. The peptide was dissolved in water and lyophilized to a powder. HPLC analysis revealed crude peptide purity as greater than 83% pure as demonstrated by area under the curve. Peptide was analyzed for molecular weight by LC-MS with an M<sup>+</sup> mass spectral analysis within equipment error. Initial results displayed an observed purity greater than 70% with an M<sup>+</sup> peak of 781, indicating the presence of a major peptide product at the desired mass.

## RESULTS & DISCUSSION

The overarching goal of this project was to create a fluorescent tag for use in studying melanoma skin cancer. A three part molecule was designed to study the hormone signaling pathway involved in malignant tumor growth. The three combined portions of the proposed molecule included a fluorescent phenanthroline-europium complex, a polyethylene glycol linker, and a melanocyte-binding peptide. The hypothesis was that this novel, three-part molecule would allow for the improved study and detection of melanoma skin cancer by creating a fluorescent lanthanide tag that does not interfere with the binding of the MSH (4) peptide by way of a modified polyethylene glycol linker, thus allowing the molecule to be taken up into the cancer cell and followed via fluorescent imagery. Currently, the three individual components of the final molecule have been synthesized and characterized.

### 3.1 PHENANTHROLINE LIGAND AND $\text{Eu}^{3+}$ COMPLEXES

#### 3.1.1 SYNTHESIS AND CHARACTERIZATION



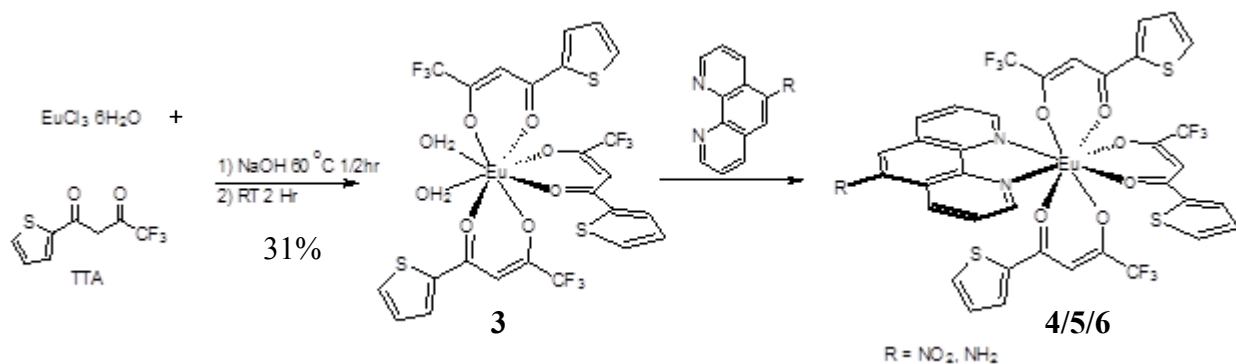
**Scheme 13.** Synthesis of 5-Amine-1, 10-Phenanthroline

5-Nitro-1,10-phenanthroline (**1**) was synthesized by the nitration of 1,10-phenanthroline. This was accomplished by heating a  $\text{HNO}_3/\text{H}_2\text{SO}_4$  solution at  $70^\circ\text{C}$  for at least 3 hours.<sup>12</sup> Yield

of the reaction was sensitive to reaction time, temperature and work-up conditions. A systematic study of these factors was not investigated. Heating the reaction mixture at reflux seemed to produce lower yields. However, the yield of the reaction seemed to improve with longer heating times. Work-up involved pouring the reaction mixture over ice and adjusting to a pH of 3 using 6M NaOH. Product precipitated as a yellow solid and was isolated by filtration. This was problematic and frequently resulted in no precipitate forming or the precipitation of large quantities of Na<sub>2</sub>SO<sub>4</sub> as a white solid. When this occurred, the Na<sub>2</sub>SO<sub>4</sub> was removed by filtration and the filtrate extracted with CH<sub>2</sub>Cl<sub>2</sub>. The reaction proceeded in adequate yields (63.5%) to produce a light yellow solid. NMR spectra of 5-nitro-1,10-phenanthroline (**1**) displayed the required singlet at  $\delta$ 8.60 as well as 2 doublet of doublets and 2 multiplets which integrated to a total of 7 hydrogens, indicating successful synthesis of the target molecule. FTIR spectra of 5-nitro-1,10-phenanthroline (**1**) showed the expected NO<sub>2</sub> stretching bands.

5-Amino-1,10-phenanthroline (**2**) was obtained following the nitration of 1,10-phenanthroline and the subsequent reduction of 5-nitro-1,10-phenanthroline (**1**). Both of these reactions were followed by NMR. The reaction proceeded smoothly and in good yields (84.3%). Reduction was accomplished using hydrazine and palladium on charcoal with ethanol as a solvent. Ethanol was degassed before use by bubbling argon through the reaction mixture before addition of the hydrazine. NMR spectra of 5-amino-1,10-phenanthroline (**2**) maintains the characteristic peaks of the 5-nitro-1,10-phenanthroline (**1**) while exhibiting a significant up-field shift as well as an additional N-H peak at  $\delta$  7.24 indicating successful ligand synthesis. FTIR spectra displayed the disappearance of the NO<sub>2</sub> stretching bands present in the starting material as well as the appearance of NH<sub>2</sub> stretching bands.

### 3.1.2 ULTRAVIOLET-VISIBLE ABSORPTION/FLUORESCENT EMISSION STUDIES



**Scheme 14.** Synthesis of Luminescent Lanthanide Complexes

Phenanthroline-lanthanide complexes were formed to obtain a luminescent profile of the proposed molecule. Complexes explored include 1,10-phenanthroline -  $\text{Eu}(\text{TTA})_3$  (**4**), 5-nitro-1,10-phenanthroline -  $\text{Eu}(\text{TTA})_3$  (**5**), and 5-amino-1,10-phenanthroline -  $\text{Eu}(\text{TTA})_3$  (**6**).

It was necessary to perform this study to determine the viability of these ligands as components of our design. Firstly  $\text{EuCl}_3(\text{H}_2\text{O})_6$  and trifluorothienyl acetone (TTA) were combined in aqueous NaOH to synthesize  $\text{Eu}(\text{TTA})_3(\text{H}_2\text{O})_2$  (**3**), collected as a white precipitant (31.2%)**Error! Bookmark not defined.** Afterward synthesis of the phenanthroline-europium complexes involved stirring the appropriate ligand with  $\text{Eu}(\text{TTA})_3(\text{H}_2\text{O})_2$  (**3**) in a mixture of methanol and chloroform overnight. The remaining solution was then filtered to yield the intended luminescent complex.

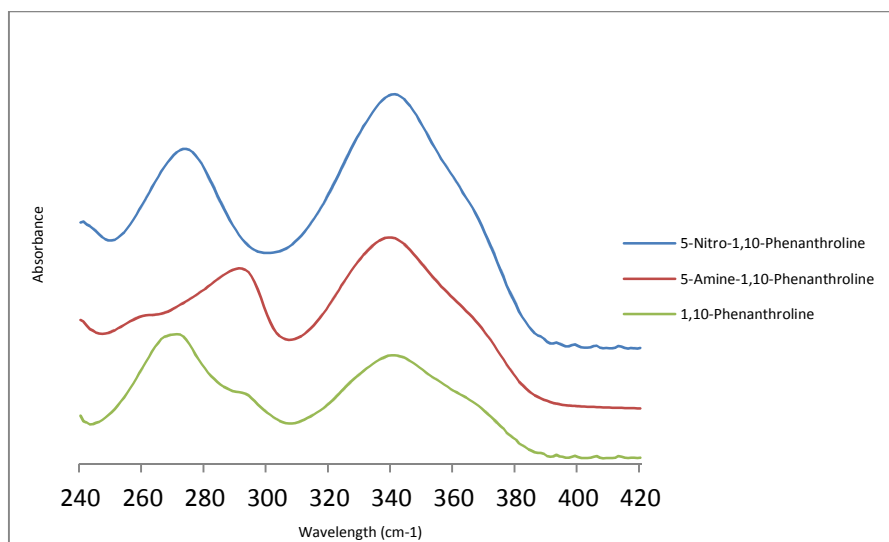


**Figure 8.** Lanthanide UV-Vis Complex Absorbance

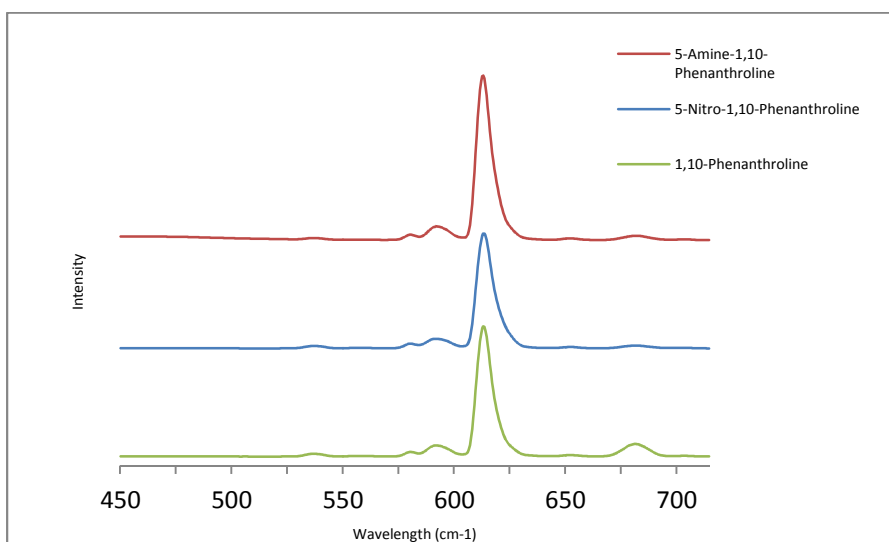
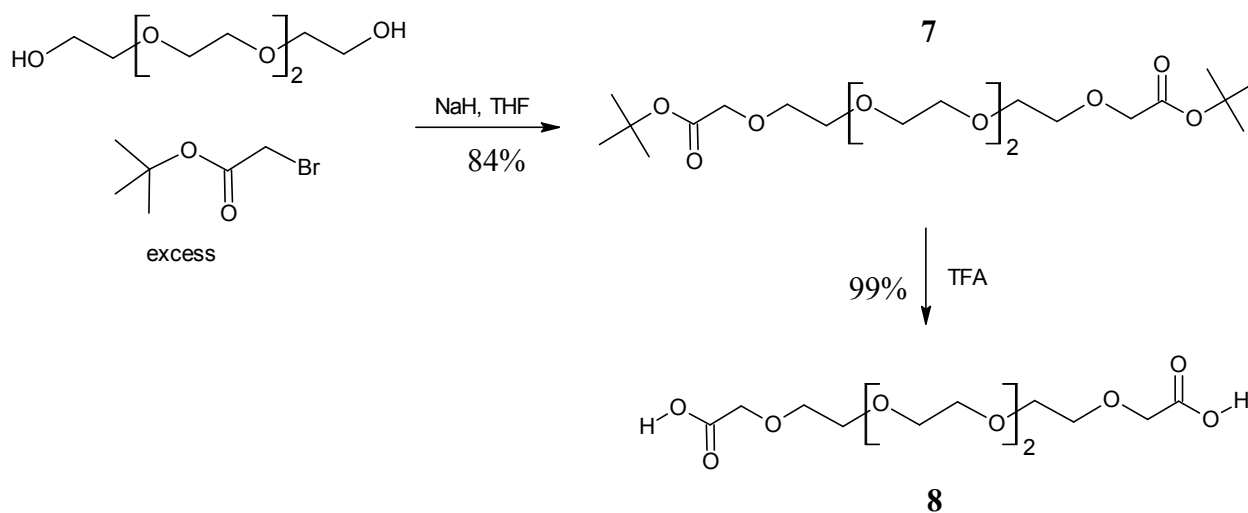


**Figure 9.** Lanthanide Complex Fluorescent Emission

Qualitative measurements for the complexes were made and quantum yields were not calculated. Absorbance max in the UV-Vis appeared at ~340 nm for all of the observed complexes (**Fig. 8**). Fluorescent spectra of the complexes showed the expected emission band at approximately ~615 nm for the europium ion (**Fig. 9**). Fluorescence spectra indicated a Stoke's shift of 275 nm while also displaying the narrow emission band of  $\text{Eu}^{3+}$ .

### 3.2 POLYETHYLENE GLYCOL LINKER



**Scheme 15.** Synthesis of the polyethylene glycol linker. Beginning with a reaction between tetraethylene glycol and t-butyl bromoacetate and concluding with the removal of the t-butyl groups in formic acid.

#### 3.2.1 SYNTHESIS AND CHARACTERIZATION

Synthesis of tert-butyl 17-hydroxy-19,19-dimethyl- 3,6,9,12,15,18-hexaoxaicosanoate (**7**) was first attempted using a literature procedure that reacted bromoacetic acid and tetraethylene glycol under basic conditions (t-butoxide). Repeated attempts failed to produce the desired product. Synthesis was successfully accomplished through the addition of tetraethylene glycol and tert-butyl bromoacetate in a solution of dry tetrahydrofuran (THF) and sodium hydride (NaH)<sup>13</sup> producing a yellow, viscous oil (**Scheme 15**).<sup>14</sup> The reaction proved difficult to reproduce reliably often producing a mixture of half reacted side product. Reaction yield appears to be very sensitive to moisture which is problematic since tetraethylene glycol is extremely hygroscopic. Using the sodium hydride in excess caused the reaction to proceed in good yields (81.79%) and high purity. It is believed that in addition to serving as a base, the

excess NaH also help dry the reaction mixture by reacting with any water that was present. Pure product was obtained once before the hydroscopic nature of tetraethylene glycol began to create a mixed product, requiring chromatography to obtain the necessary purity. NMR spectra displayed the characteristic 4 hydrogen singlet at  $\delta$ 3.94. FTIR absorbance bands for the t-butyl ester were also diagnostic for monitoring the reaction. Observed peaks include 2979, 2870, 1747, 1366, 1224, 1120, 945, 844, & 746  $\text{cm}^{-1}$ .

To remove the terminal t-butyl groups, tert-butyl 17-hydroxy-19,19-dimethyl-3,6,9,12,15,18-hexaoxaicosanoate (**7**) was dissolved in formic acid, yielding 2-hydroxy-1 $\lambda^3$ ,4,7,10,13,16-hexaoxaoctadec-1-yn-18-oic acid (**8**) as a yellow oil in high yield (99%)<sup>14</sup> (**Scheme 15**). The reaction proceeded smoothly and quantitatively. NMR spectra displayed a carboxylic acid peak at  $\delta$ 10.24, the diagnostic 4 hydrogen peak at  $\delta$ 4.16, and the removal of the terminal t-butyl groups. FTIR analysis of the diacid revealed the presence of the diagnostic peaks found in the starting material while also displaying the presence of a carboxylic acid –OH stretch at 3125  $\text{cm}^{-1}$ .

### 3.2.4 GCMS & HPLC STUDIES

GCMS was performed to monitor reaction progress of the synthesis of tert-butyl 17-hydroxy-19,19-dimethyl-3,6,9,12,15,18-hexaoxaicosanoate (**7**) and determine final purity. The reaction was characterized by the gradual disappearance of the starting material at retention time 10.479 min and the appearance of the product peak at a retention time of 16.879 min. Purity was determined to be greater than 93% as demonstrated by area under the curve. MS was highly fragmented due to the use of electron impact ionization, gas ionization would likely provide a less fragmented spectra.

HPLC was performed to follow the synthesis of 2-hydroxy-1 $\lambda^3$ ,4,7,10,13,16-hexaoxaoctadec-1-yn-18-oic acid (**8**) and to determine resulting purity. GC could not be used since the diacid did not move well on the GC column. HPLC analysis displayed a purity of greater than 93% with a retention time of 2.449 min (mobile phase: 90% H<sub>2</sub>O/10% CH<sub>3</sub>CN).

### 3.3 MELANOCYTE STIMULATING HORMONE (4) - PG

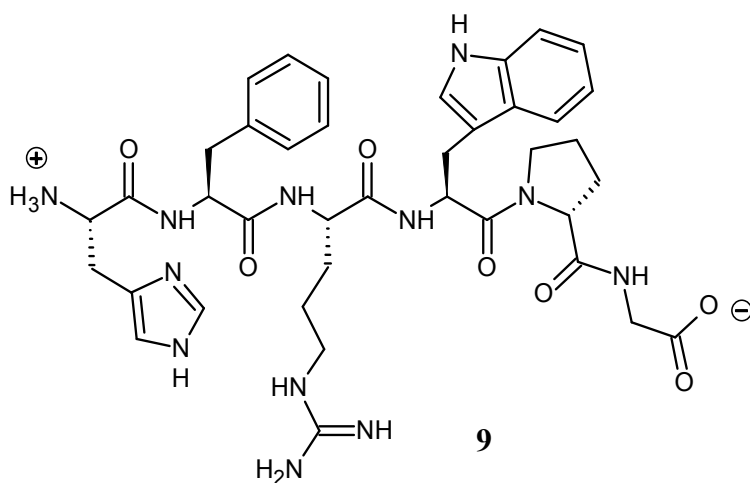


**Figure 10.** Melanocyte Stimulating Hormone (4) - PG

#### 3.3.1 SOLID PHASE SYNTHESIS & CHARACTERIZATION

Microwave assisted solid phase peptide synthesis was performed using an adapted CEM Mars6 microwave with fiber optic probe. The provided temperature probe was disassembled in order that the fiber optic probe could be placed directly into the reaction vessel, ensuring proper heating and allowing reactions to be completed in quick succession. Synthesis was performed on a Rink amide resin, sequentially adding amino acids until completion of the targeted peptide chain.<sup>10,15</sup> Cleavage was performed on bench top due to the corrosive nature of TFA and the metal interior of the Mars6 microwave. A sealed, non-reactive reaction vessel would be required



to complete microwave assisted cleavage. Peptide was analyzed for molecular weight by LC-MS with an M+1 mass spectral analysis within equipment error (**Fig. 11**). Initial results displayed an observed purity greater than 70% with an M<sup>+1</sup> peak of 781, indicating the presence of a major peptide product at the desired mass (**Fig. 12**).

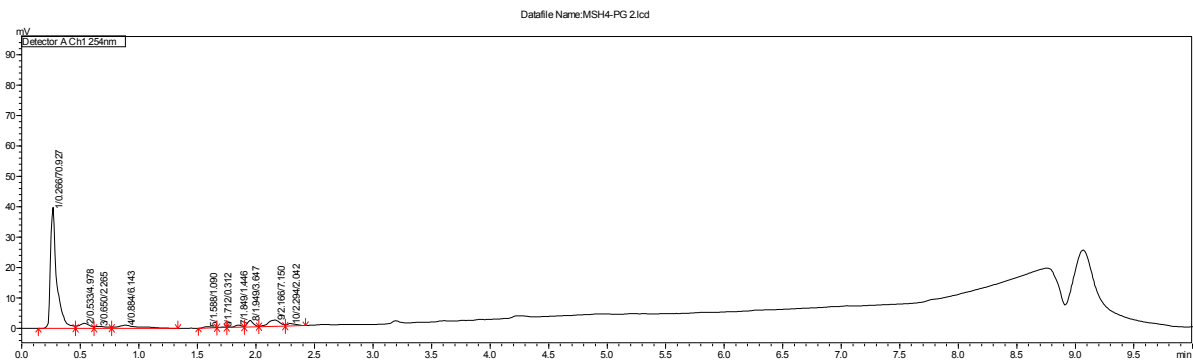


**Figure 11.** LCMS of MSH (4)-PG

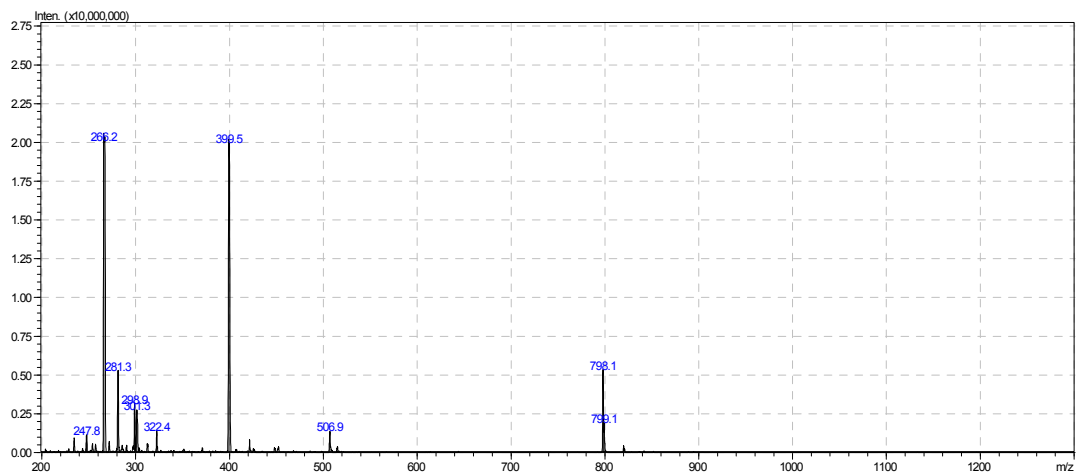


**Figure 12.** Mass Spectra of MSH (4)-PG

Due to the low retention time of the peptide in the LCMS chromatogram, additional HPLC was performed to confirm the previous results. HPLC analysis revealed crude peptide purity as greater than 90% pure as demonstrated by area under the curve, confirming the presence of a major peptide product (**Fig. 13**).

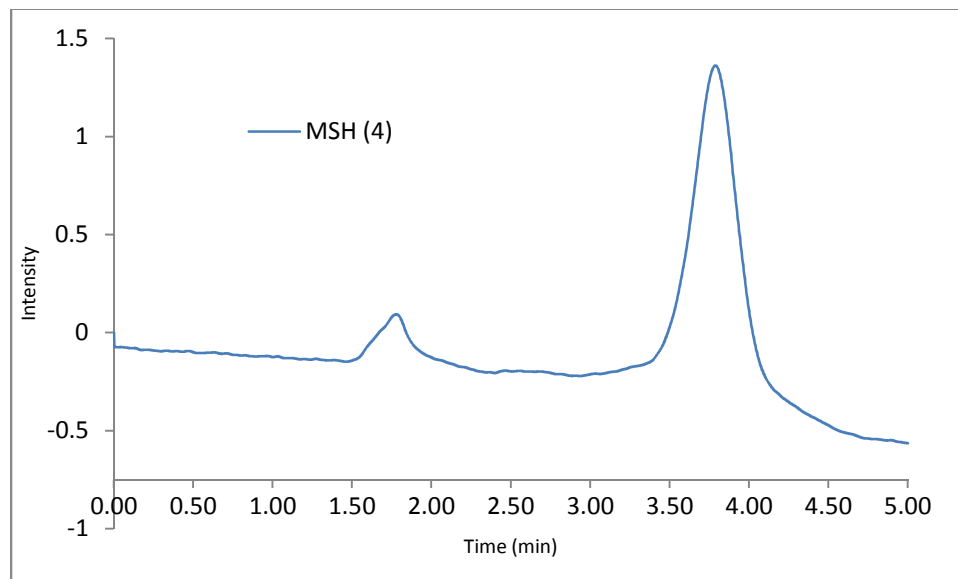


**Figure 13.** HPLC Chromatogram of MSH (4) - PG

### 3.4 CONCLUSION

Currently synthesis and characterization of the project's three required components has been completed. The functionalized phenanthroline ligand (**2**) was first synthesized from 1,10-phenanthroline and characterized using NMR. Ligand-lanthanide complexes (**4,5,6**) were subsequently synthesized and qualitatively analyzed via UV-Vis/Fluorescent spectroscopy to determine their viability as luminescent tags. Intense emission at ~615 nm after excitation at ~340 nm qualitatively indicated a viable luminescent tag. Following completion of the

functionalized ligand, a polyethylene glycol linker was synthesized from tetraethylene glycol and t-butyl bromoacetate (**8**). NMR characterization and GCMS studies indicated successful linker synthesis. Next a MSH(4)-PG peptide (**10**) was synthesized using a microwave assisted solid phase protocol. LCMS and HPLC analysis revealed a major peptide product with purity greater than 90% at the desired mass, indicating successful synthesis. The project's conclusion involved the combination of the three individual components (**2,8,10**), which was first attempted by the addition of the modified polyethylene glycol linker (**8**) to the functionalized phenanthroline ligand (**2**) through the creation of an acid chloride intermediate (**9**). This reaction was determined to be unsuccessful after several attempts using various combinations of reaction conditions and solvent systems.

### 3.5 FUTURE WORK

Additional work required to continue project synthesis includes: combination of the phenanthroline ligand and the polyethylene glycol linker, attachment of the linker-ligand molecule to the peptide on solid phase resin, cleavage and purification of the completed molecule, formation of the lanthanide chelate, and subsequent fluorescent studies.

Attempts to complete the final molecule proved difficult as various solubility issues prevented successful synthesis. This being mentioned, future attempts at synthesis of the proposed molecule must overcome solubility issues involved in the combination of the modified polyethylene glycol linker and the phenanthroline ligand. Once this first combinatory step is accomplished, synthesis of the final molecule should follow without further difficulty.

SUPPLEMENTAL MATERIAL

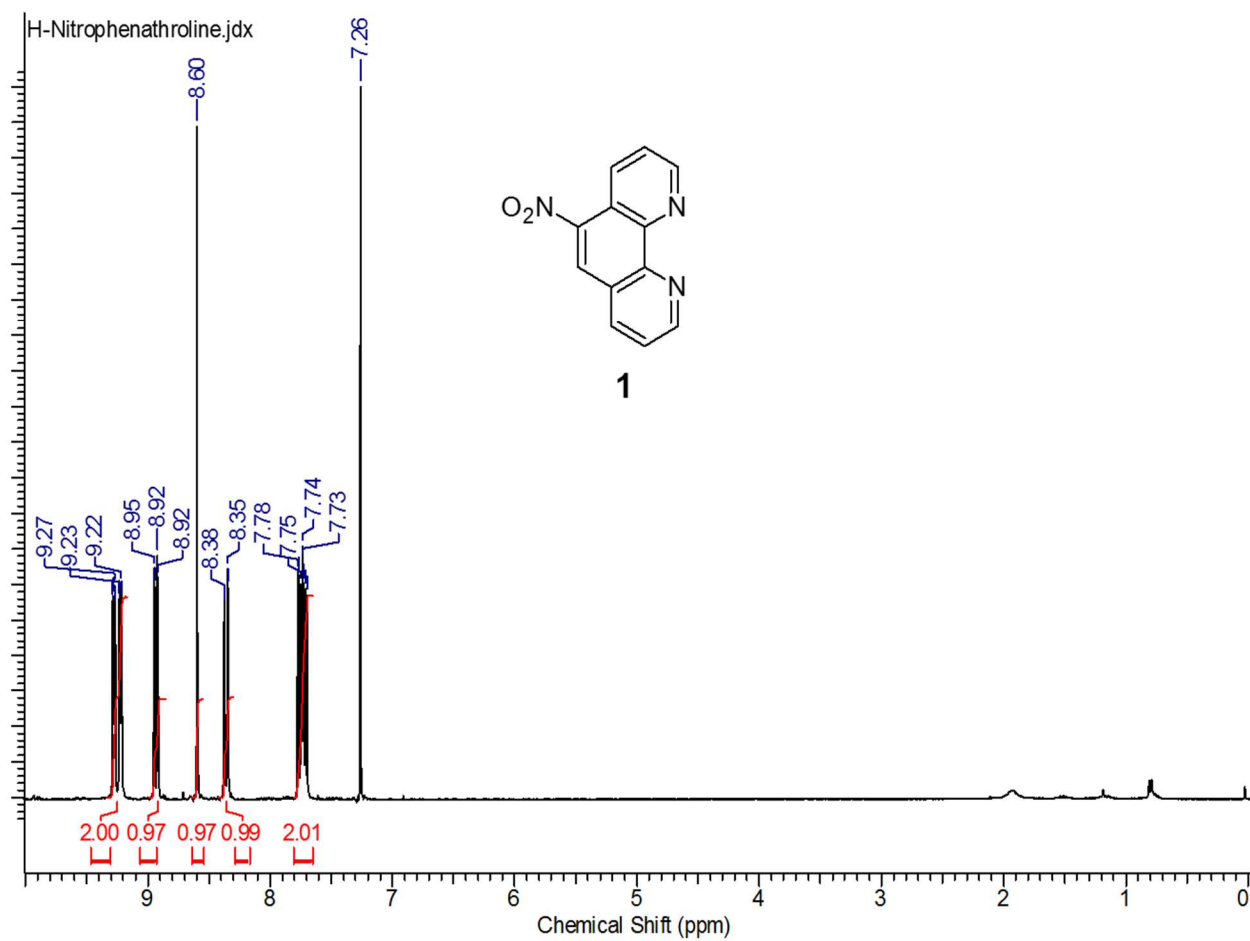


**Figure 14.**  $^1\text{H}$  NMR spectrum of 5-Nitro-1,10-Phenanthroline in  $\text{CDCl}_3$

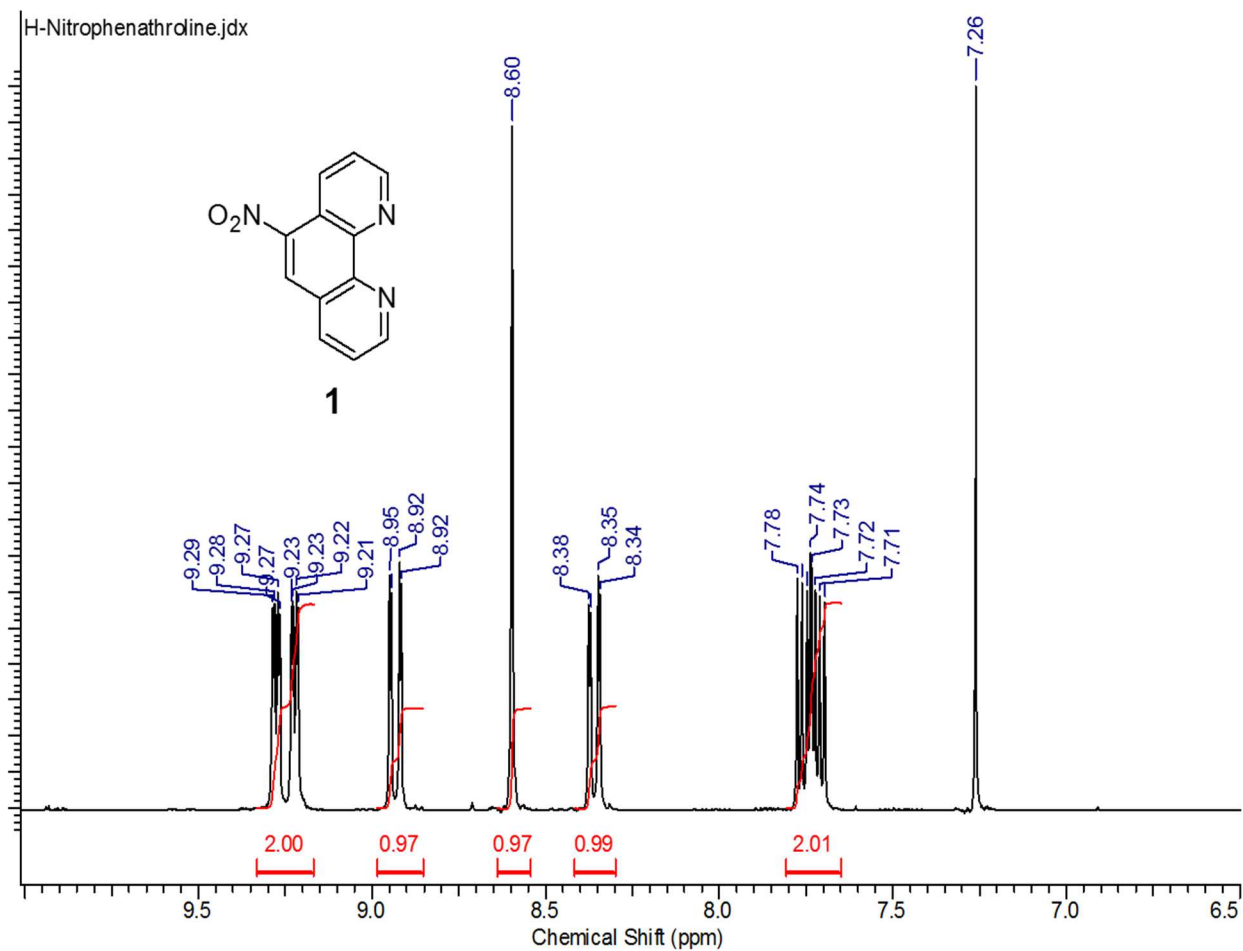


**Figure 15.** Zoomed  $^1\text{H}$  NMR spectrum of 5-Nitro-1,10-Phenanthroline in  $\text{CDCl}_3$

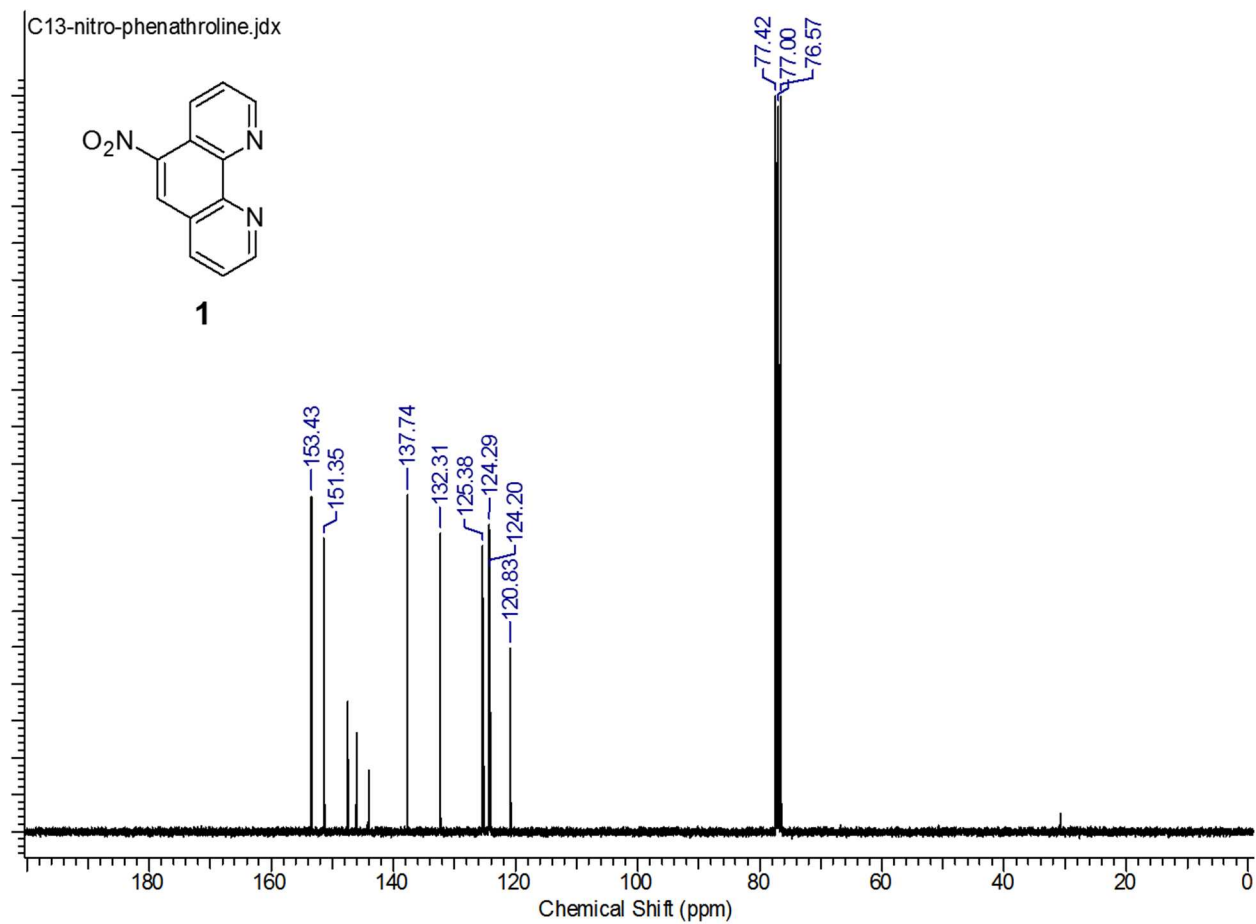


**Figure 16.** C13 NMR spectrum of 5-Nitro-1,10-Phenanthroline in CDCl<sub>3</sub>

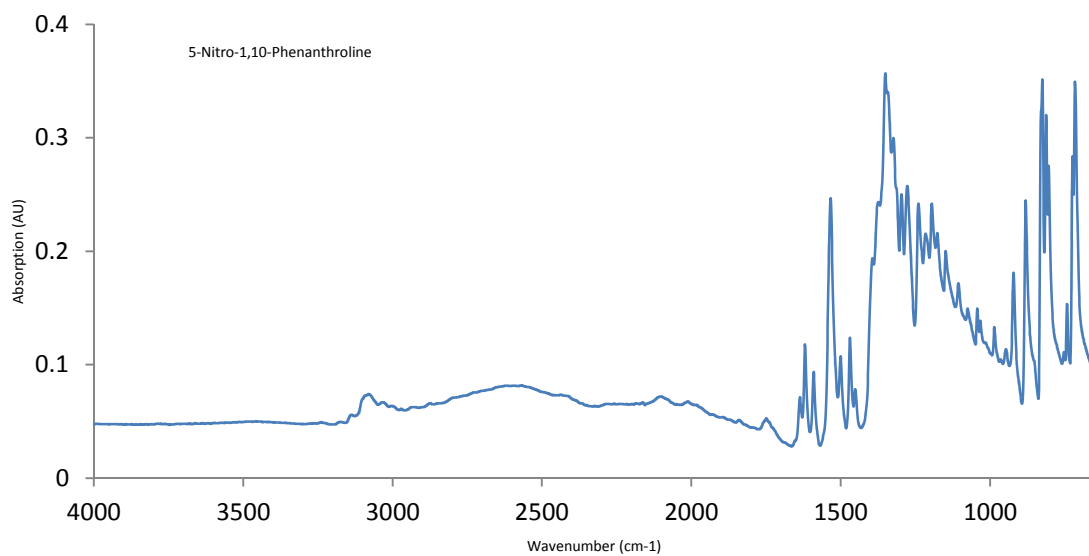


**Figure 17.** FTIR spectrum of 5-Nitro-1,10-Phenanthroline.

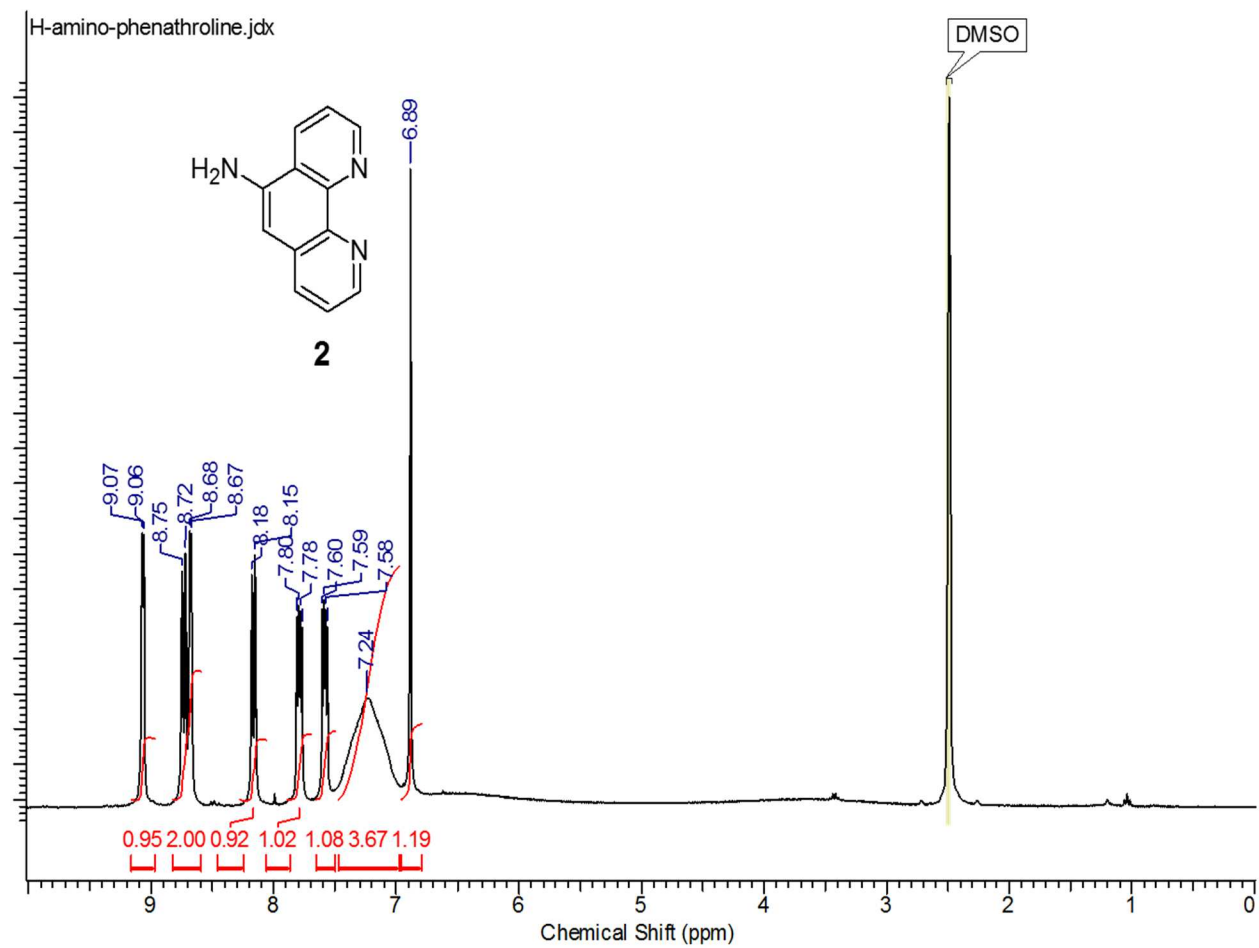


**Figure 18.**  $^1\text{H}$  NMR spectrum of 5-Amine-1,10-Phenanthroline in DMSO.



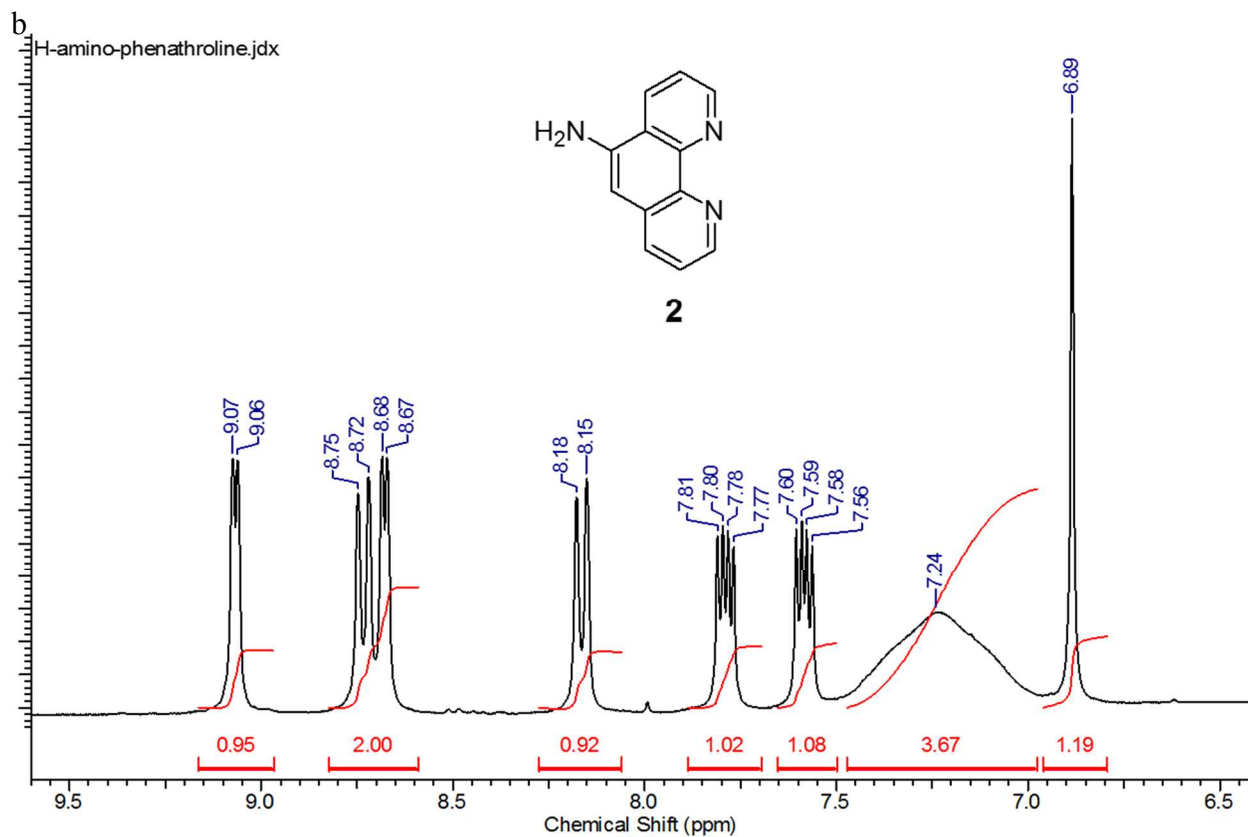


**Figure 19.** Zoomed  $^1\text{H}$  NMR spectrum of 5-Amine-1,10-Phenanthroline in DMSO.

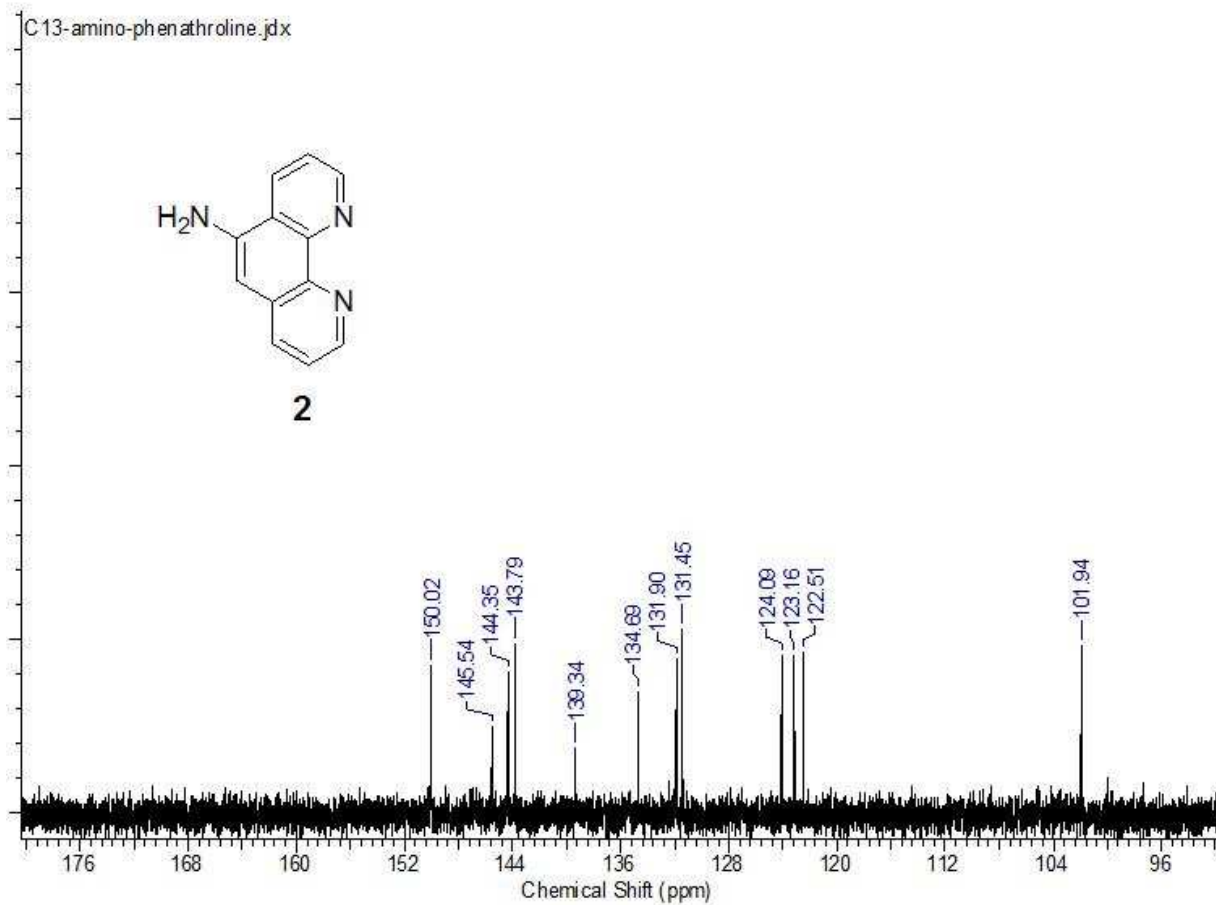


**Figure 20.** C13 NMR spectrum of 5-Amine-1,10-Phenanthroline in DMSO.

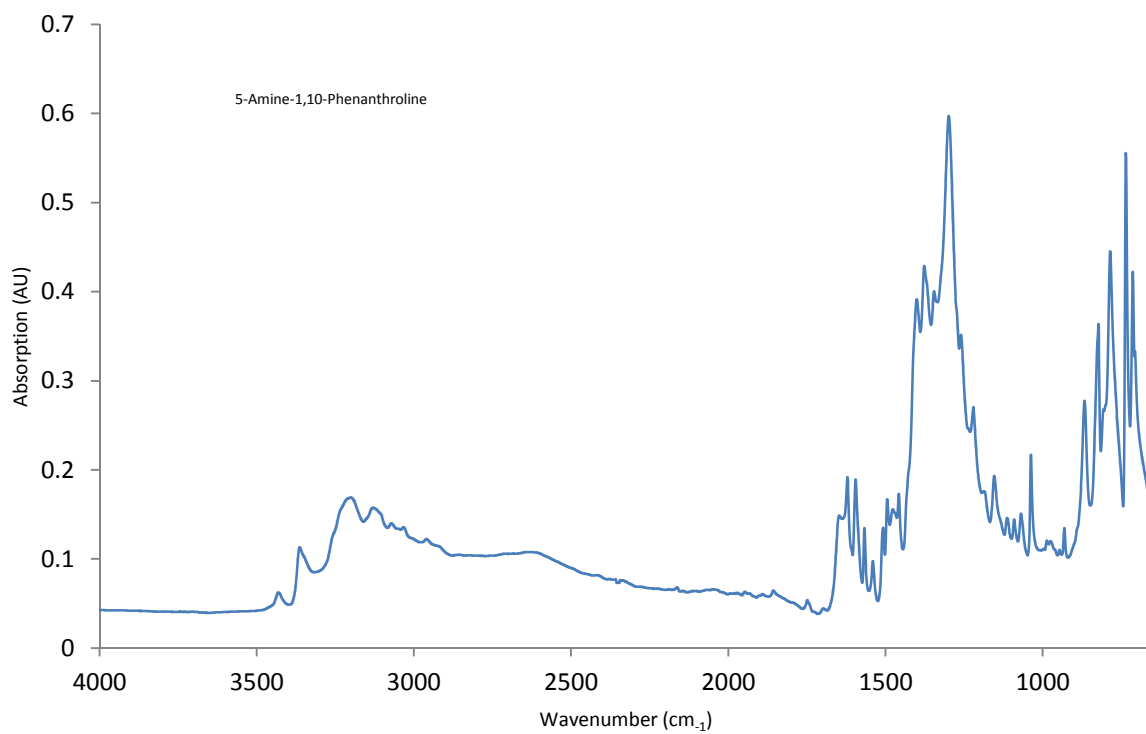


**Figure 21.** FTIR spectrum of 5-Amine-1,10-Phenanthroline.

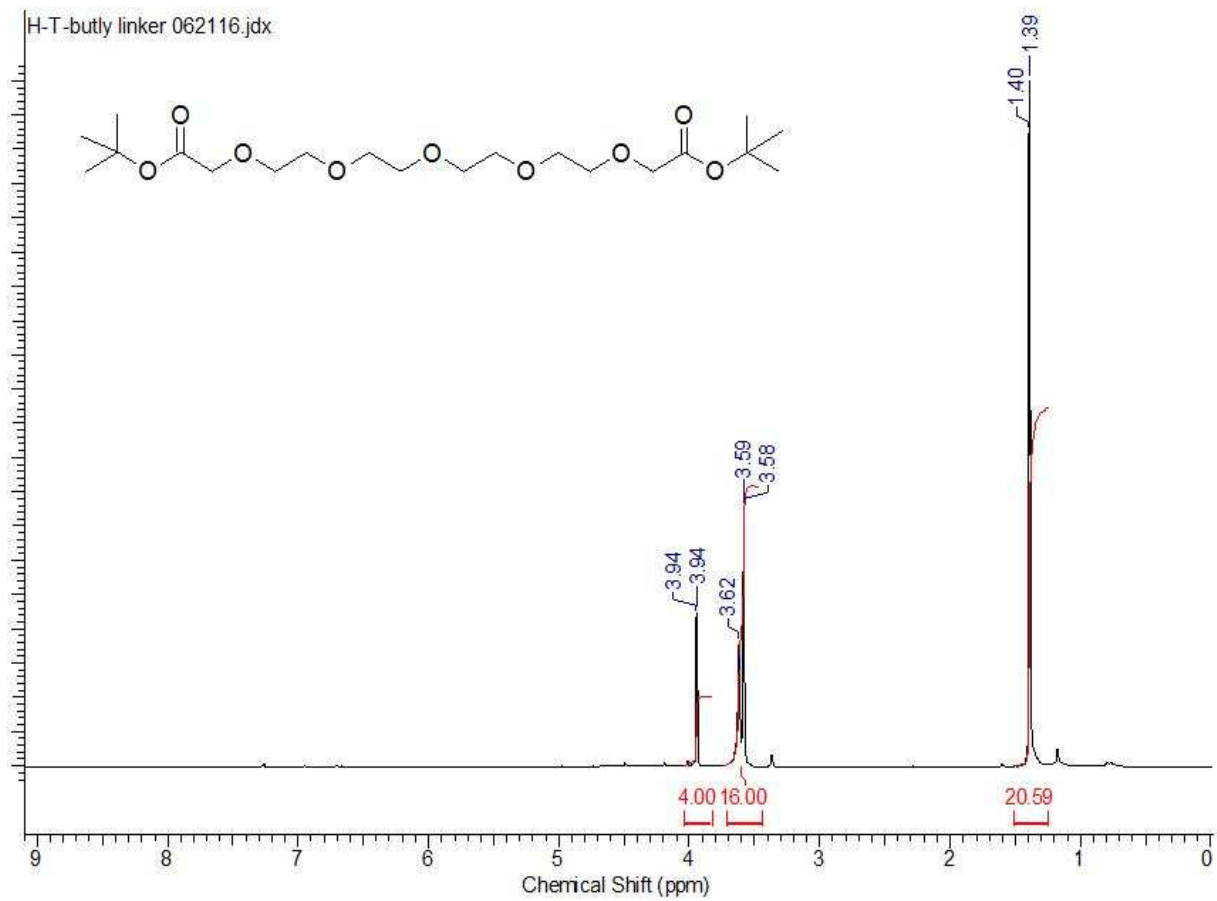


**Figure 22.**  $^1\text{H}$  NMR spectrum of tert-butyl 17-hydroxy-19,19-dimethyl-3,6,9,12,15,18-hexaoxaicosanoate in  $\text{CDCl}_3$ .



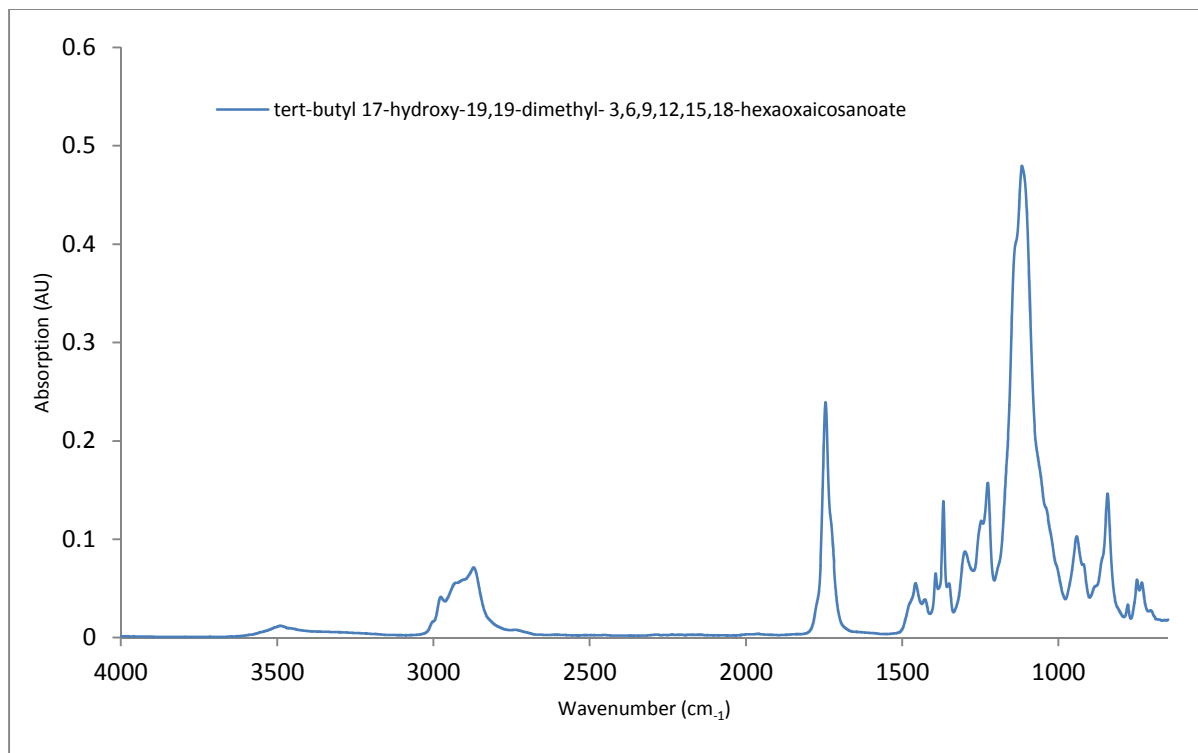


**Figure 24.** FTIR spectrum of tert-butyl 17-hydroxy-19,19-dimethyl-3,6,9,12,15,18-hexaoxaicosanoate.

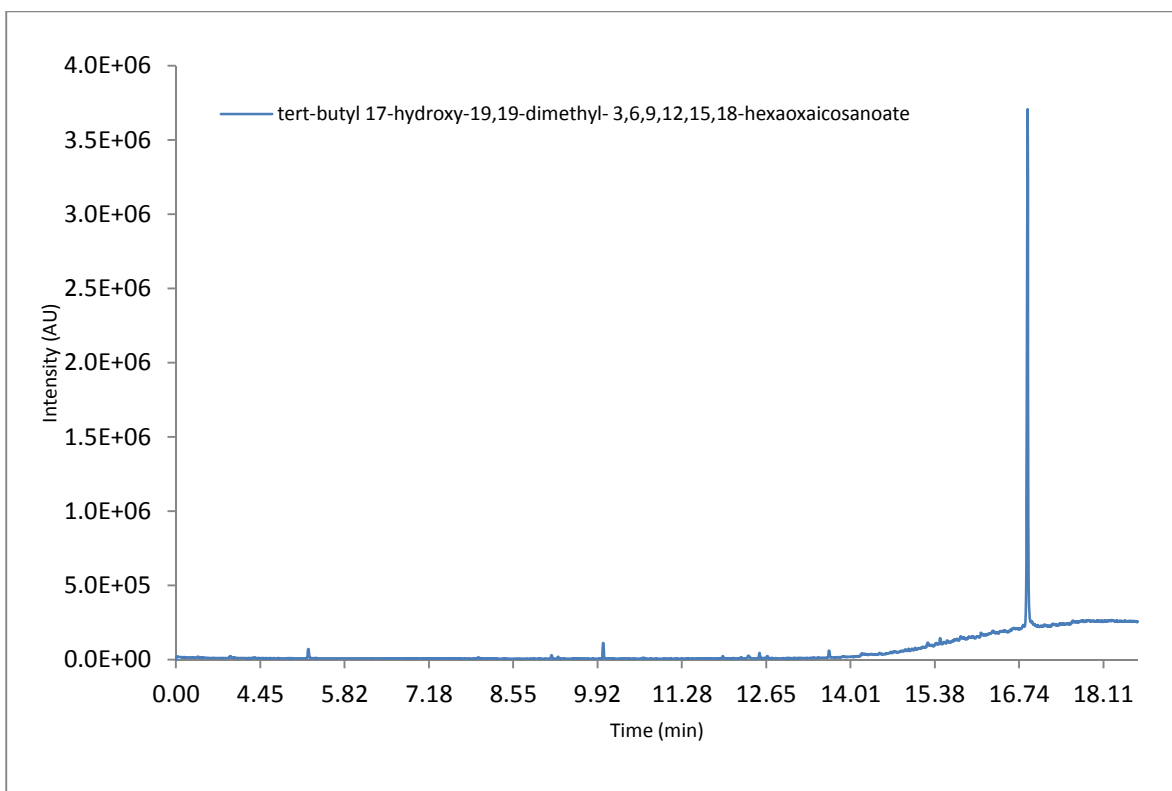


**Figure 25.** GCMS chromatogram of tert-butyl 17-hydroxy-19,19-dimethyl-3,6,9,12,15,18-hexaoxaicosanoate.







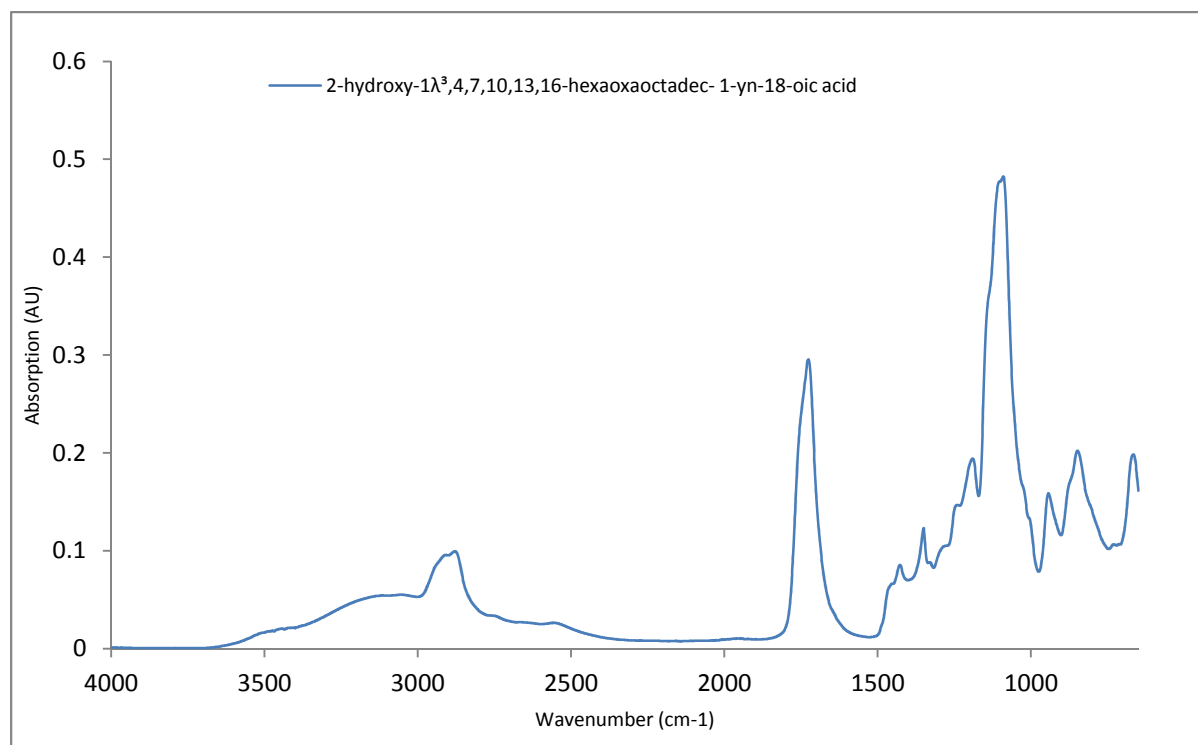


**Figure 28.** FTIR spectrum of 2-hydroxy-1λ³,4,7,10,13,16- hexaoxaoctadec- 1-yn-18-oic acid.

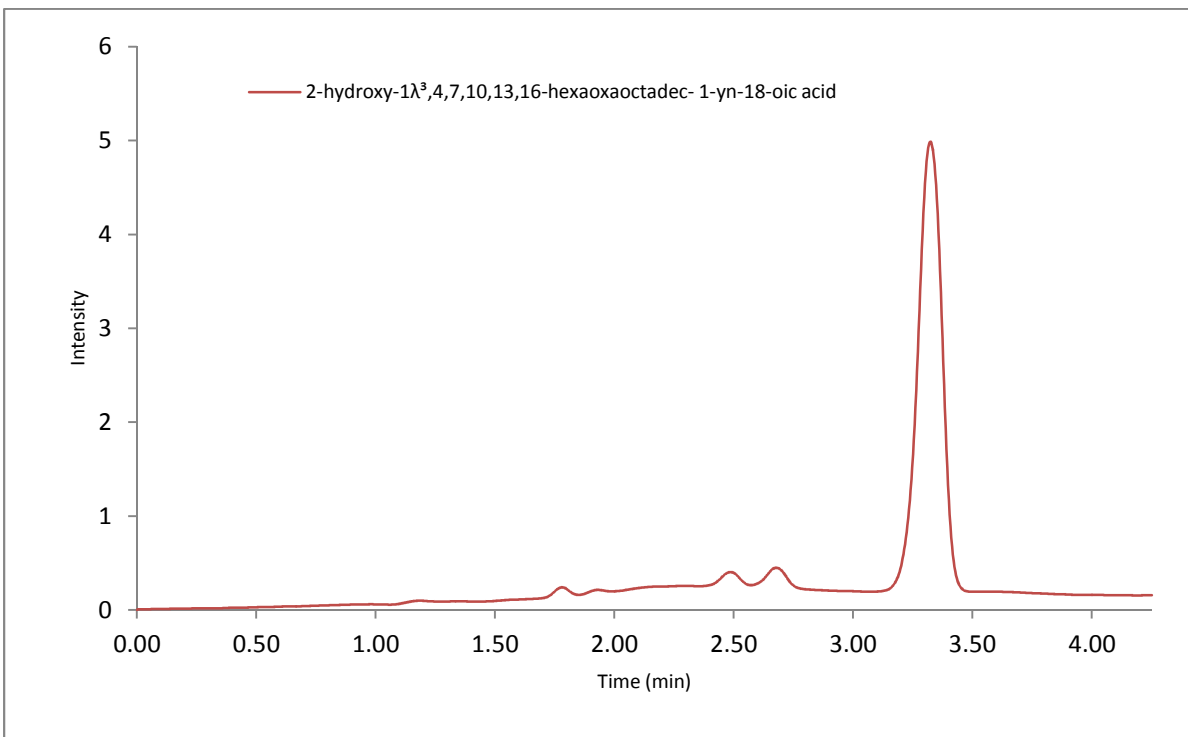


**Figure 29.** HPLC chromatogram of 2-hydroxy-1λ<sup>3</sup>,4,7,10,13,16- hexaoxaoctadec- 1-yn-18-oic acid.

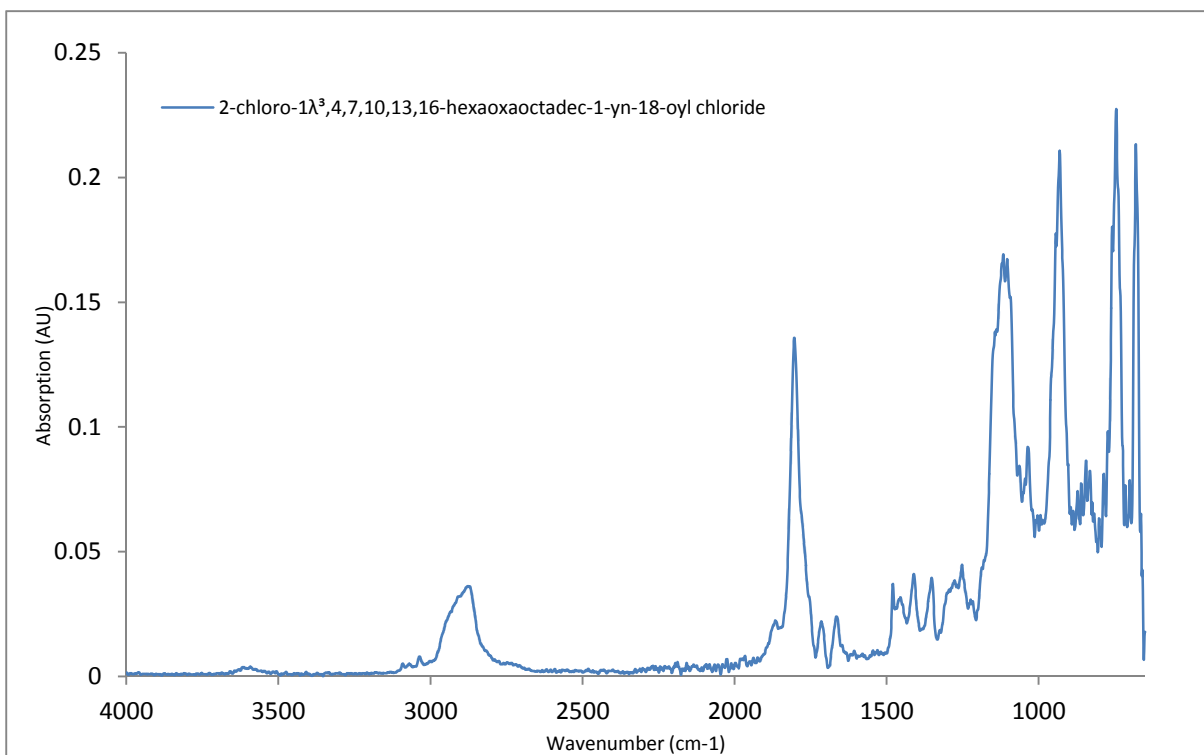


**Figure 30.** FTIR spectrum of 2-chloro-1λ³,4,7,10,13,16-hexaoxaoctadec-1-yn-18-oyl chloride.

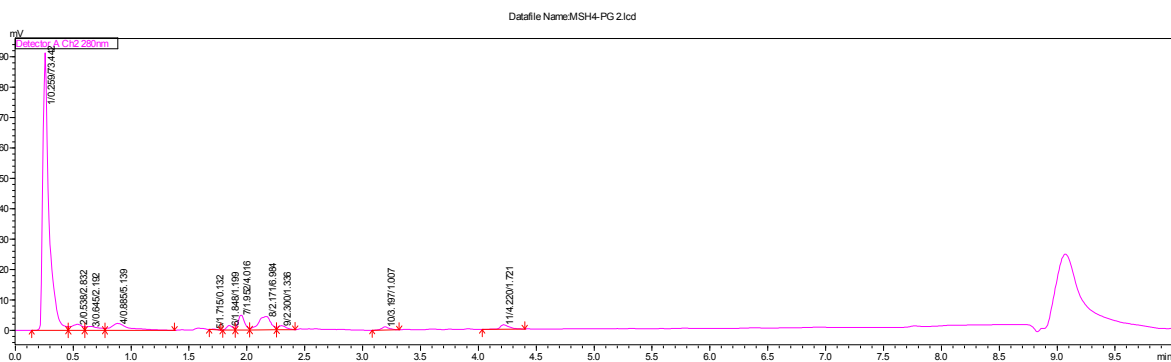


**Figure 31.** LC chromatogram of MSH(4)-PG

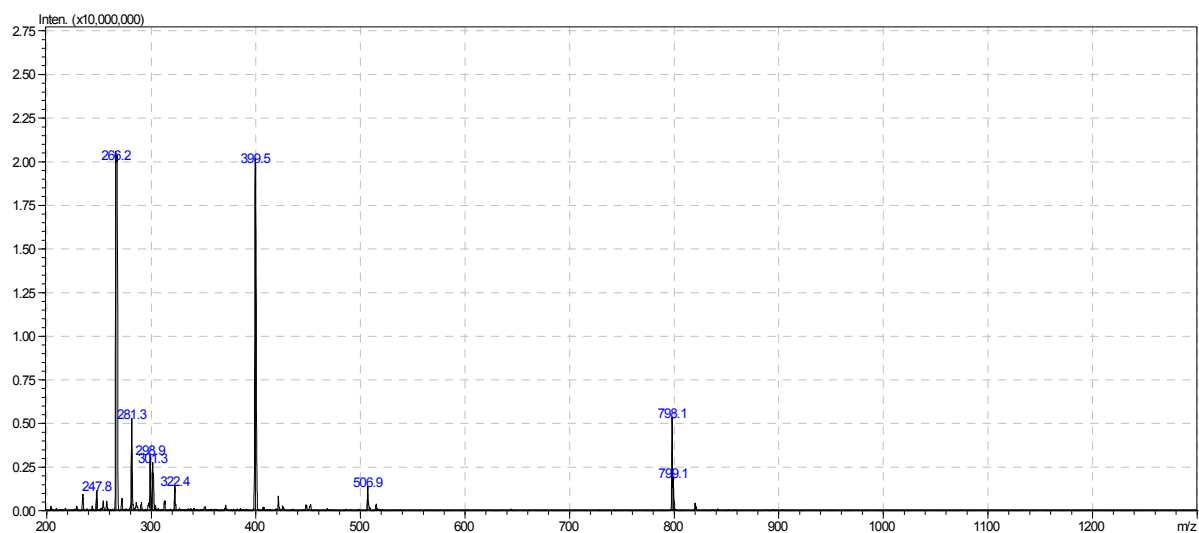


**Figure 32.** Mass spectra of MSH(4)-PG

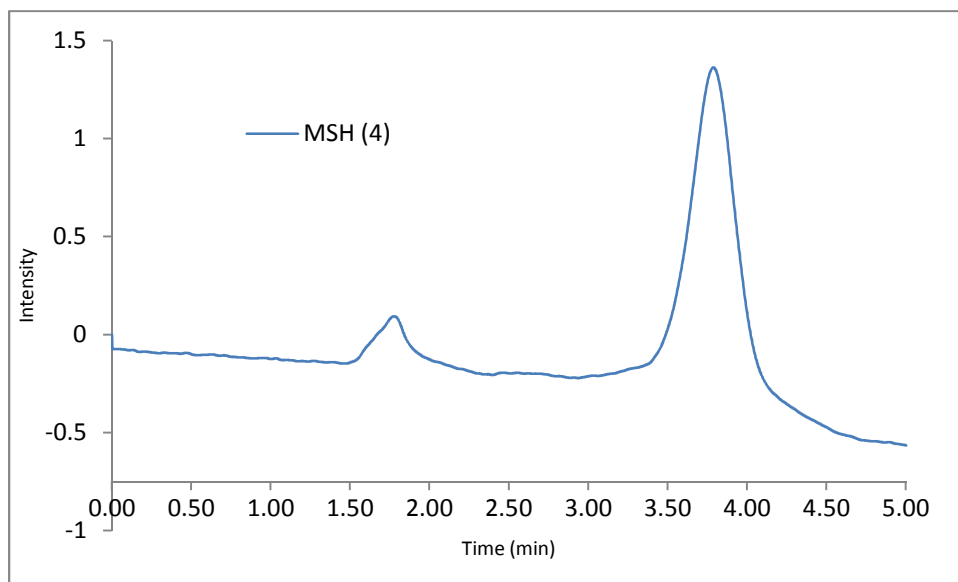


**Figure 33.** HPLC chromatogram of MSH(4)-PG

## APPENDIX A - PERMISSIONS

### Figure 2

A G-Protein Coupled Receptor activating a cell's signaling pathway through the presence of an agonist (signaling molecule)

|                                 |   |
|---------------------------------|---|
| License Number                  | 3962860730440   |
| License date                    | Oct 06, 2016  |
| Licensed Content<br>Publisher   | Nature Publishing Group   |
| Licensed Content<br>Publication | Nature  |
| Licensed Content Title          | The Molecule Pages database   |
| Licensed Content Author         | Joshua Li, Yuhong Ning, Warren Hedley, Brian Saunders,<br>Yongsheng Chen et al. |
| Licensed Content Date           | Dec 12, 2002  |
| Licensed Content Volume         | 420   |
| Licensed Content Issue          | 6916  |

## REFERENCES

- <sup>1</sup> Ramesh Alleti, Josef Vagner, Dilani Chathurika Dehigaspitiya, Valerie E. Moberg, N. G. R. D. Elshan, Narges K. Tafreshi, Nabila Brabez, Craig S. Weber, Ronald M. Lynch, Victor J. Hruby, Robert J. Gillies, David L. Morse, Eugene A. Mash. Synthesis and Characterization of Time-resolved Fluorescence Probes for Evaluation of Competitive Binding to Melanocortin Receptors. *J. Bioorg. Med. Chem.* 2013, 21, 5029-5038.
- <sup>2</sup> Beasley J. Synthesis, Characterization, and Luminescent Properties of Eu<sup>3+</sup> Dipyridophenazine Functionalized Complexes for Potential Bio-Imaging Applications. M.S. Thesis *Western Carolina University*, 2014.
- <sup>3</sup> Ma, Y.; Wang Y. Recent advances in the sensitized luminescence of organic europium complexes. *Coordin. Chem. Rev.* **2010**, 254, 972–990.
- <sup>4</sup> *World Cancer Report 2014*. World Health Organization. 2014. pp. Chapter 5.14.
- <sup>5</sup> National Cancer Institute. US Department of Health & Human Services. *The Basal Layer*. <http://training.seer.cancer.gov/melanoma/anatomy/layers.html>.
- <sup>6</sup> P. Ciarletta, L. Foret, M. Ben Amar. The radial growth phase of malignant melanoma: multi-phase modelling, numerical simulations and linear stability analysis. *J. R. Soc. Interface* 2011, 8, 345-368..
- <sup>7</sup> Lee, Hwa Jin; Wall, Brian; Chen, Suzie. G-Protein Coupled Receptors and Melanoma. *Melanoma* Susan Lehman Cullman Laboratory for Cancer Research, Department of Chemical Biology, Ernest Mario School of Pharmacy, Rutgers University. *Cell Melanoma Res.* 2008 Aug;21(4):415-28.
- <sup>8</sup> Li, Joshua; Ning, Yuhong; Hedley, Warren; Saunders, Brian; Chen, Yongsheng; Tindill, Nicole; Hannay, Timo; Subramaniam, Shankar. The Molecule Pages Database. *Nature December 2002*, **420**, 716-717.
- <sup>9</sup> Hagan A.K; T. Zuchner. Lanthanide-based time-resolved luminescence immunoassays *Anal Bioanal Chem* 2011, 400,2847–2864.
- <sup>10</sup> De Silva, Channa R.; Vagner, Josef; Lynch, Ronald; Gillies, Robert J.; Hruby, Victor J. Optimization of Time-Resolved Fluorescence Assay for Detection of Europium-Tetraazacyclododecyltetraacetic Acid-Labeled Ligand-receptor interactions. *Anal. Biochem.* 2010 Mar 1;398(1):15-23.
- <sup>11</sup> Divya, V.; Sankar, V.; Raghu, K.G.; Reddy, M.L.P. A mitochondria-specific visible-light sensitized europium  $\beta$ -diketonate complex with red emission. *Dalton T.* **2013**, 42, 12317.
- <sup>12</sup> Ji, Shaomin; Guo, Huimin; Yuan, Xiaolin; Li, Xiaohuan; Ding, Haidong; Gao, Peng; Zhao, Chunxia; Wu, Wenting; Wu, Wanhua; Zhao, Jianzhang. A Highly Selective OFF-ON Red-Emitting Phosphorescent Thiol Probe with Large Stokes Shift and Long Luminescent Lifetime. *Org. Let.* 2010 Vol. 12, No. 12 2876-2879
- <sup>13</sup> Wittman, Valentin; Shuichi Takayama; Gong, Kei Wei; Weitz-Schmidt, Gabriele; Wong, Chi-Huey. Ligand Recognition by E- and P-Selectin: Chemoenzymatic Synthesis and Inhibitory Activity of Bivalent Sialyl Lewis x Derivatives and Sialyl Lewis x Carboxylic Acids. *J. Org. Chem.* 1998, 63, 5137-5143
- <sup>14</sup> Simeone, Luca; Mangiapia, Gaetano; Vitiello, Giuseppe; Irace, Carlo; Colonna, Alfredo; Ortona, Ornella; Montesarchio, Daniela; Paduano, Luigi. Cholesterol-Based Nucleolipid-Ruthenium Complex Stabilized by Lipid Aggregates for Antineoplastic Therapy. *Bioconjugate Chem.* 2012 February 28, 758–770.



---

<sup>15</sup> Pescatore, Robyn; Marrone, Gina F.; Sedberry, Seth; Vinton, Daniel; Finkelstein, Netanel; Katlowitz, Yitzhak E.; Pasternak, Gavril W.; Wilson, Krista R.; Majumdar, Susruta. Synthesis and Pharmacology of Halogenated  $\delta$ -Opioid-Selective [D-Ala<sup>2</sup>]Deltorphan II Peptide Analogues. *ACS Chem Neurosci*. 2015 June 17; 6(6): 905–910.